TURUN YLIOPISTON JULKAISUJA
ANNALES UNIVERSITATIS TURKUENSIS

SARJA - SER. A I OSA - TOM. 456

ASTRONOMICA - CHEMICA - PHYSICA - MATHEMATICA

SUPERNOVAE IN DENSE AND DUSTY ENVIRONMENTS

by

Erkki Kankare

TURUN YLIOPISTO
UNIVERSITY OF TURKU
Turku 2013

From

Department of Physics and Astronomy
University of Turku
FI-20014 Turku
Finland

Supervised by

Dr. Seppo Mattila
Department of Physics and Astronomy
University of Turku
Finland

Reviewed by

Prof. Juri Poutanen
Astronomy Division
Department of Physics
University of Oulu
Finland

Dr. Dovi Poznanski
School of Physics and Astronomy
Tel Aviv University
Israel

Opponent

Dr. Bruno Leibundgut
European Southern Observatory
Germany

ISBN 978-951-29-5291-5 (PRINT)
ISBN 978-951-29-5292-2 (PDF)
ISSN 0082-7002
Painosalama Oy - Turku, Finland 2013

Acknowledgements

First of all a big thank you to my supervisor Seppo Mattila who introduced me to supernovae and relentlessly guided me through my long PhD process and never stopped listening to his student who so often walked into his office to bother him.

Many thanks too to my MSc supervisor Pekka Teerikorpi who introduced me into making science in the first place. I would also like to thank Stuart Ryder for the very successful collaboration on the Gemini programme, and Stefano Benetti for including me in the ESO/NTT Large Programme. Similar thanks go to Rubina Kotak, Peter Lundqvist, Andrea Pastorello, Miguel Ángel Pérez-Torres, Cristina Romero-Cañizales, Jason Spyromilio, Stefano Valenti, Petri Väisänen and all the other colleagues with whom I have had the honour to work, but who are unfortunately far too many to name here. Special thanks go to Ricardo Cardenes and Kaj Wiik for spending so much of their time to save mine, by solving my many computer problems. I am also grateful to all the staff and students of Tuorla Observatory for creating such a pleasant work environment.

I also want to thank Johannes Andersen and Thomas Augusteijn for having me as a student support astronomer at the Nordic Optical Telescope for a year and a half. A great thanks also to the telescope staff and students, I think we had fun.

I thank the pre-examiners of this thesis, Prof. Juri Poutanen and Dr. Dovi Poznanski, for their useful comments, and Dr. Bruno Leibundgut for agreeing to be my opponent at the public defense. I thank the Finnish Academy of Science and Letters, the Nordic Optical Telescope Science Association, the G. W. Wulff foundation and the University of Turku foundation for their financial support of the work included in this thesis. I also thank John Datson for the language correction of this thesis.

And a big thanks to my mother and father for all their support, suuri kiitos äidille ja isälle kaikesta tuesta. And last but certainly not least, thanks to my love Juliet - you smile the light into my darkness.

Contents

Abstract

In this doctoral thesis supernovae in dense and dusty environments are studied, with an emphasis on core-collapse supernovae. The articles included in the thesis aim to increase our understanding of supernovae interacting with the circumstellar material and their place in stellar evolution. The results obtained have also importance in deriving core-collapse supernova rates with reliable extinction corrections, which are directly related to star formation rates and galaxy evolution. In other words, supernovae are used as a tool in the research of both stellar and galaxy evolution, both of which can be considered as fundamental basics for our understanding of the whole Universe.

A detailed follow-up study of the narrow-line supernova 2009kn is presented in paper I, and its similarity to another controversial transient, supernova 1994W, is shown. These objects are clearly strongly interacting with relatively dense circumstellar matter, however their physical origin is quite uncertain. In paper I different explosion models are discussed.

Discoveries from a search programme for highly obscured supernovae in dusty luminous infrared galaxies are presented in papers II and III. The search was carried out using laser guide star adaptive optics monitoring at near-infrared wavelengths. By comparing multi-band photometric follow-up observations to template light curves, the likely types and the host galaxy extinctions for the four supernovae discovered were derived.

The optical depth of normal spiral galaxy disks were studied statistically and reported in paper IV. This is complementary work to studies such as the one presented in paper V, where the missing fractions of core-collapse supernovae were derived for both normal spiral galaxies and luminous infrared galaxies, to be used for correcting supernova rates both locally and as a function of redshift.

List of publications

I SN 2009kn - the twin of the Type IIn supernova 1994W,
E. Kankare, M. Ergon, F. Bufano, J. Spyromilio, S. Mattila, N. N. Chugai, P. Lundqvist, A. Pastorello, R. Kotak, S. Benetti, M-T. Botticella, R. J. Cumming, C. Fransson, M. Fraser, G. Leloudas, M. Miluzio, J. Sollerman, M. Stritzinger, M. Turatto, S. Valenti (2012), MNRAS, 424, 855 [arXiv:1205.0353]

II Discovery of a Very Highly Extinguished Supernova in a Luminous Infrared Galaxy,
E. Kankare, S. Mattila, S. Ryder, M.-A. Pérez-Torres, A. Alberdi, C. Romero-Canizales, T. Díaz-Santos, P. Väisänen, A. Efstathiou, A. Alonso-Herrero, L. Colina, J. Kotilainen (2008), ApJ, 689, L97 [arXiv:0810.2885]

III Discovery of Two Supernovae in the Nuclear Regions of the Luminous Infrared Galaxy IC 883,
E. Kankare, S. Mattila, S. Ryder, P. Väisänen, A. Alberdi, A. Alonso-Herrero, L. Colina, A. Efstathiou, J. Kotilainen, J. Melinder, M.-A. Pérez-Torres, C. Romero-Cañizales, A. Takalo (2012) ApJ, 744, L19 [arXiv:1112.0777]

IV Revisiting the optical depth of spiral galaxies using the Tully-Fisher B relation,
E. Kankare, M. Hanski, G. Theureau, P. Teerikorpi (2009), A&A, 493, 23 [arXiv:0810.4773]

V Core-collapse supernovae missed by optical surveys,
S. Mattila, T. Dahlen, A. Efstathiou, **E. Kankare**, J. Melinder, A. Alonso-Herrero, M. Á. Pérez-Torres, S. Ryder, P. Väisänen, G. Östlin (2012), ApJ, 756, 111 [arXiv:1206.1314]

List of abbreviations

AGB - asymptotic giant branch
AO - adaptive optics
BSG - blue supergiant
CCSN - core-collapse supernova
CDS - cool dense shell
CSM - circumstellar matter
ECSN - electron-capture supernova
FOV - field-of-view
FWHM - full width at half maximum
GRB - gamma-ray burst
IMF - initial mass function
IR - infrared
ISM - interstellar matter
LBV - luminous blue variable
LGS - laser guide star
LIRG - luminous infrared galaxy
NGS - natural guide star
OIS - Optimal Image Subtraction
PISN - pair-instability supernova
PSF - point spread function
RSG - red supergiant
SFR - star formation rate
SN - supernova
SNR - supernova rate
ULIRG - ultraluminous infrared galaxy
VLBI - very-long-baseline interferometry
WD - white dwarf
WR - Wolf-Rayet
ZAMS - zero age main sequence

Chapter 1

Introduction

New 'stars' appearing in the sky have fascinated people since historical times. First written records of these Galactic supernovae (SNe) date back as far as 185 AD with naked eye observations made by Chinese astronomers. Since then several other Galactic SNe have been observed, including such famous historical SNe as SN 1006 and SN 1054, which were visible for some time even in daylight. Nowadays modern instruments at astronomical observatories enable astronomers to study these events in detail in other galaxies, even at cosmological distances.

Stars are spherical concentrations of gas in an equilibrium of the inward pushing gravity of the stars own mass and the outward pushing radiation and thermal pressure powered by nuclear fusion. Some of the stars end their life cycles in a SN explosion, ejecting a significant fraction of their mass into space. Depending on their explosion mechanisms, SNe are divided into two main categories: core-collapse SNe (CCSNe) from massive stars, and thermonuclear SNe from white dwarf (WD) stars in binary systems.

Due to the significant brightness of SN explosions, they can be used as important tools to study the Universe. The well predictable evolution of so-called Type Ia SN explosions has enabled their calibration to be used as 'standard candles' to measure cosmological distances, which also led to the discovery of the accelerating expansion of the Universe, the work that was awarded the 2011 Nobel Prize in Physics.

While the thermonuclear SNe originate from older stellar populations, the progenitors of CCSNe are thought to be massive stars with relatively short lifetimes of up to a few tens of millions of years. Therefore, the explosion rates of CCSNe can be used to directly and independently trace the on-going star formation in their host galaxies, which is a key element in the current and future studies of the galaxy evolution. This will be partic-

ularly important at high redshift, where rapidly star forming galaxies start to dominate the overall star formation. In fact, the evolution of galaxies at high redshift is included in the key science points of the next generation astronomical observatories, such as the European Extremely Large Telescope (E-ELT) or the *James Webb Space Telescope* (*JWST*). SN observations in the local Universe can be used to study the dust extinction effects on observed SN rates (SNRs), in order to correct these SNRs and hence also star formation rates (SFRs) at large distances, which requires better understanding of SNe in dense and dusty environments.

In Chapter 2 different SN explosion models are briefly introduced and in Chapter 3 different CCSN types are summarized, with an emphasis on SNe interacting with circumstellar matter (CSM). A description of dust and extinction obscuring SNe is given in Chapter 4. An insight on SN searches and rates are given in Chapter 5. A summary of the articles included in the thesis is given in Chapter 6 and plans of future work presented in Chapter 7.

Chapter 2

Supernova explosions

While burning hydrogen, most stars belong to the main sequence. If the stars are massive enough, after hydrogen burning they will start a helium burning phase and evolve away from the main sequence. Fig. 2.1 presents a Hertzsprung-Russell diagram of stars where the $B-V$ colour and V-band absolute magnitude of a selection of main-sequence, giant and WD stars are plotted. With more massive stars that burn hydrogen more efficiently, this evolution away from the main sequence takes place faster. Stars roughly in the range of $\sim$10$-$30 $M_\odot$ evolve into K and M type red supergiants (RSGs) and even more massive O-type stars evolve via a luminous blue variable (LBV) phase into Wolf-Rayet (WR) stars. These stars are thought to be the main progenitors of CCSNe.

However, characteristics such as metallicity, stellar rotation and in particular mass-loss, all affect the stellar evolution. Mass-loss rates and wind velocities of RSGs can be of the order of $\sim 10^{-5} - 10^{-4}$ $M_\odot$ yr^{-1} and $\sim 10 - 100$ km s^{-1}, respectively (Dwarkadas 2005; Kotak & Vink 2006); and of WR stars $\sim 10^{-8} - 10^{-5}$ $M_\odot$ yr^{-1} and $\sim 1000 - 3000$ km s^{-1}, respectively (Dwarkadas 2005; Crowther 2007). For comparison, in LBVs the wind properties can differ significantly between quiescence and relatively short eruptive phases with the mass-loss rates being in the range $\sim 10^{-7} - 10^{-4}$ $M_\odot$ yr^{-1} and wind velocities ranging between $\sim 100 - 500$ km s^{-1} (Humphreys & Davidson 1994; Leitherer 1997; Kotak & Vink 2006) or even close to ~ 1000 km s^{-1} (Pastorello et al. 2010). The mass-loss history of the progenitor star can have a significant effect on the type of the resulting CCSN. Furthermore, the interaction of the SN ejecta with the CSM can also affect the observed display of the SN.

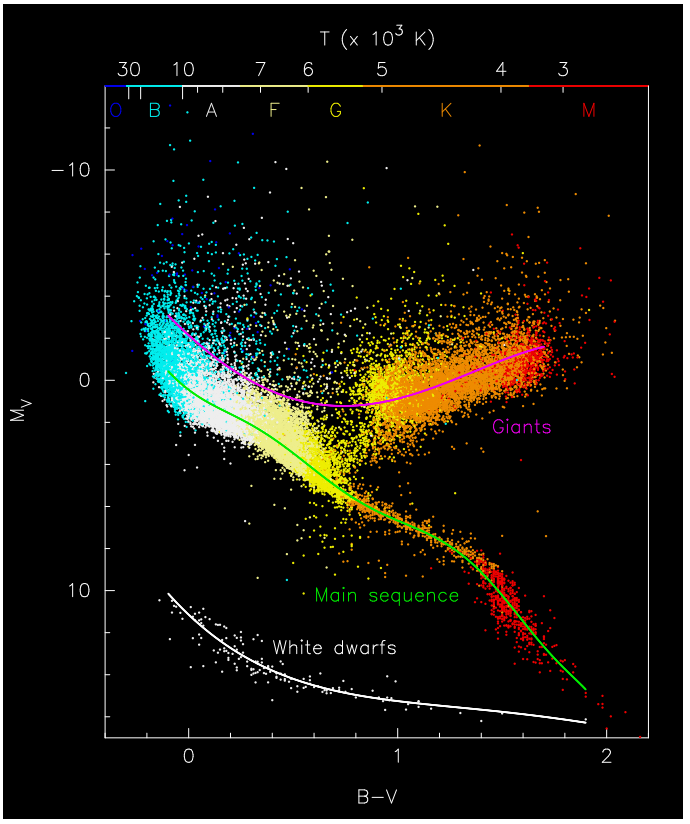

Figure 2.1: Hertzsprung-Russell (colour − absolute magnitude) diagram of main sequence, giant and WD stars plotted from the Hipparcos catalogue (Perryman et al. 1997) (excluding stars with a standard error of trigonometric parallax > 0.09 mas and a standard error on $B - V$ colour > 0.02 mag) and the preliminary 3rd version Gliese catalogue of nearby stars (Gliese & Jahreiß 1991) via VizieR (Ochsenbein et al. 2000). The main sequence temperature axis is calculated from the colour, based on the empirical model of Flower (1996). Commonly used stellar spectral classes O, B, A, F, G, K, M are marked in the upper part of the plot.

2.1 Iron-core-collapse supernovae

Following the hydrogen and helium burning in the core, the nuclear burning of the most massive stars will evolve further with subsequent burning phases of the fusion products of the previous stages in the core, in the order of carbon, neon, oxygen and silicon. In the final stages these stars will have developed an iron core. When the mass of the iron core reaches the so-called Chandrasekhar mass ($M_{ch} = 1.4$ M$_\odot$) the gravitational force within the core surpasses the electron degeneracy pressure and the core collapses with relativistic velocities. When the core reaches high enough densities of $\rho \sim 10^{14}$ g cm^{-3} a shock wave from a core bounce decelerates the collapse (e.g. the review of Janka et al. 2007). This is followed by a luminous SN explosion driven by a neutrino burst, ejecting the outer parts of the star into space. However, the exact details of the explosion mechanisms are still uncertain. In the normal iron core collapse the approximate total energy release, deposited as a short burst of neutrinos created in the dense core, is $\sim 10^{53}$ erg (e.g. Smartt 2009). From this a canonical energy of $\sim 10^{51}$ erg (i.e. $\sim$1 %) is reabsorbed as the kinetic energy of the outer parts of the star (i.e. the SN ejecta) (Janka et al. 2007). The efficiency of converting kinetic energy into luminosity is $\sim$1$-$10 % corresponding to a total integrated radiation energy of $\sim 10^{49}-10^{50}$ erg (Smartt 2009). The core is thought to collapse into a compact remnant, either a neutron star or a black hole, directly or with a delay.

In the SN explosion numerous radioactive elements are synthesized (see Table 2.1), with ^{56}Ni, ^{57}Ni and ^{44}Ti having the most significant effect on the visible light curve. The typical amount of ^{56}Ni synthesized in an iron-core collapse can be up to $\sim$1 M$_\odot$. The initial peak of most of the CCSN light curves is powered by the radioactive decay $^{56}\mathrm{Ni} \rightarrow {}^{56}\mathrm{Co}$ followed by the light curve tail phase dominated by the $^{56}\mathrm{Co} \rightarrow {}^{56}\mathrm{Fe}$ decay (e.g. Arnett 1979; Colgate et al. 1980; Barbon et al. 1984). The mean lifetime τ (i.e. the e-folding time of a radioactive element) is a way to describe the radioactive decay

$$\tau = \frac{t_{1/2}}{\ln 2}, \tag{2.1}$$

where $t_{1/2}$ is the half-life. The luminosity $L(t)$ at time t powered by the radioactive decay is proportional to the initial luminosity L_0 and the e-

folding time of the decay (see e.g. Arnett 1982)

$$L(t) = L_0 e^{-t/\tau} \tag{2.2}$$

and the magnitude change to the change in the luminosity

$$\Delta m = -2.5 \log(\frac{L}{L_0}). \tag{2.3}$$

Radioactive ^{56}Co has an e-folding time of $\tau_{\rm Co} = 111.26$ days. Therefore the theoretical decline rate for the tail phase of a SN powered by the radioactive decay of ^{56}Co is 0.976 mag (100 days)$^{-1}$, assuming complete γ-ray and e^+ trapping in the ejecta. If this can be assumed, the mass of radioactive ^{56}Ni synthesized in the core-collapse can be estimated by scaling the tail phase luminosity directly with that of the famous Type IIP SN 1987A (see Chapter 3.1)

$$M(^{56}\mathrm{Ni})_{\rm SN} = \frac{L_{\rm SN}}{L_{\rm 87A}} M(^{56}\mathrm{Ni})_{\rm 87A}, \tag{2.4}$$

which had an observed tail phase consistent with theoretical ^{56}Co decay (Bouchet et al. 1991).

SN 1987A exploded in the Large Magellanic Cloud and has thus been the closest SN so far observed with modern instruments, making it the best studied SN and thus an ideal object for comparison. For example Bouchet et al. (1991) estimated the radioactive ^{56}Ni mass for SN 1987A to be $M(^{56}\mathrm{Ni})_{\rm 87A} = 0.069$ M$_\odot$. However, the bolometric SN light curve in the tail phase can deviate from the expected radioactive decay tail, e.g. if γ-rays and e^+ are not completely trapped or if the SN ejecta is interacting with the surrounding CSM and the interaction contributes significantly to the light curve.

The other radioactive elements mentioned above, decay via $^{57}\mathrm{Ni} \rightarrow {}^{57}\mathrm{Co} \rightarrow {}^{57}\mathrm{Fe}$ and $^{44}\mathrm{Ti} \rightarrow {}^{44}\mathrm{Sc}$, and, for example in the case of SN 1987A, ^{57}Co and ^{44}Ti became the dominant sources of luminosity at day $\sim$1100$-$1200 and $\sim$1700$-$1800 respectively (Woosley et al. 1989; Diehl & Timmes 1998; Fransson & Kozma 2002; Grebenev et al. 2012).

Table 2.1: Most important radioactive decay processes powering the SN light curves, adapted from Diehl & Timmes (1998).

Isotope		Decay products	Decay process	τ_e
^{56}Ni	$\rightarrow$	^{56}Co + γ	e^- capture	8.8 days
^{56}Co	$\rightarrow$	^{56}Fe + γ	e^- capture	111.3 days
^{56}Co	$\rightarrow$	^{56}Fe + e^+	e^+ decay	
^{56}Fe		-	stable	-
^{57}Ni	$\rightarrow$	^{57}Co + γ	e^- capture	52 hours
^{57}Co	$\rightarrow$	^{57}Fe + γ	e^- capture	390 days
^{57}Fe		-	stable	-
^{44}Ti	$\rightarrow$	^{44}Sc + γ	e^- capture	$\sim$89 years
^{44}Sc	$\rightarrow$	^{44}Ca + γ	e^- capture	5.4 hours
^{44}Sc	$\rightarrow$	^{44}Ca + e^+	e^+ decay	
^{44}Ca		-	stable	-

In the very late phases, the SN light curve can also turn into a very slow decline powered by light echoes from the interstellar matter (ISM), as observed, for example, in the case of the Type IIL SN 1980K (Sugerman et al. 2012) or in the case of the Type Ia SN 1998bu (Cappellaro et al. 2001). For different SN types, see Chapter 3.

2.2 Electron-capture supernovae

The main pre-SN path of massive ($\gtrsim 8$ M$_\odot$) stars is nuclear burning, forming an iron core, followed by its collapse. An alternative model has been suggested for *some* CCSNe having so-called super asymptotic giant branch (AGB) star progenitors with initial masses close to the core-collapse limit ($\sim 8 - 10$ M$_\odot$). These stars could already experience a collapse of the core at the O/Ne/Mg stage and explode as so-called electron-capture SNe (ECSNe) (Miyaji et al. 1980). To summarize the model: Although the core mass increases towards the Chandrasekhar mass by carbon burning,

the mass and temperature are not high enough for neon burning to be ignited in the degenerate core (e.g. Nomoto 1984, 1987). As the core has become electron degenerate, the electron capture of ^{24}Mg and/or ^{20}Ne decreases the electron pressure, increasing the core density and triggering the collapse of the core when the central density reaches $\sim 1-4\times10^{9}$ g cm^{-3} (e.g. Miyaji & Nomoto 1987; Gutiérrez et al. 2005).

The simulations of Kitaura et al. (2006) conclude a low explosion energy for ECSNe and consequently low synthesized ^{56}Ni mass < 0.015 M$_{\odot}$. Similarly, the simulations of Mayle & Wilson (1988) and Wanajo et al. (2009) have suggested even lower ^{56}Ni mass estimates of only $\sim 0.002-0.0045$ M$_{\odot}$ for ECSN events. However, a below average explosion energy does not necessarily result in an ECSN with low observed luminosity. If the super-AGB star has experienced a significant mass ejection episode before the core-collapse (see Poelarends et al. 2008), due, for example to Mira-type pulsations (Hashimoto et al. 1993) which can be expected for such stars, it can lead to a high maximum luminosity caused by the SN ejecta-CSM interaction. In fact, Weaver & Woosley (1979) suggest that a super-AGB star could lose its whole hydrogen envelope due to instability with a maximum velocity of $\sim$100 km s^{-1}.

ECSNe from super-AGB stars have been suggested to explain the nature of a variety of transient events with relatively low spectral line velocities and the inferred ^{56}Ni masses for core-collapse events. These transients range from low-luminosity ($-12 \gtrsim M_{R,\max} \gtrsim -15$) events such as SN 2008S (Prieto et al. 2008; Botticella et al. 2009) to the peculiar bright ($M_{R,\max} \approx -18$) Type IIP SN 2007od interacting with a CSM (Inserra et al. 2011).

2.3 Pair-instability supernovae

Models for very massive stars in the range of $\sim$100$-$260 M$_{\odot}$ predict temperature and density conditions ($\rho \lesssim 10^{6}$ g cm^{-3}, $T \gtrsim 10^{9}$ K; Waldman 2008) that trigger an $e^- + e^+$ pair production at the end of the carbon-burning phase (see e.g. Heger & Woosley 2002; Woosley et al. 2002; Heger et al. 2003), which leads to a drop in thermal radiation pressure, partial collapse, instability and events of major mass loss. In the mass range of $\sim$100$-$140 M$_{\odot}$ pulsational pair-instability events eject matter from the outer layers of the star, followed by the core likely collapsing into a black hole (Heger & Woosley 2002; Heger et al. 2003). In the mass range of

$\sim$140$-$260 $M_\odot$ it is expected that only one major pulsation occurs that completely destroys the progenitor star in a pair-instability SN (PISN) event, leaving no remnant (i.e. neutron star or black hole) (Heger & Woosley 2002; Heger et al. 2003). The mass ranges given by the models above are associated with low metallicity, but parameters such as metallicity and rotation can be expected to affect these ranges (Heger et al. 2003). The models predict a variety of luminosities for PISNe depending on the amount of hydrogen still bound to the progenitor at the time of the explosion and the ejected ^{56}Ni mass. The total explosion energies predicted by the models can be up to $\sim 10^{53}$ erg, similar to the ordinary iron-core-collapse SNe, with ^{56}Ni, however, being synthesized up to $\sim$50 $M_\odot$ (Heger et al. 2003). Similarly, the pulsational pair-instability events can also be very luminous if the pulsations take place closely after one another and the ejected shells interact with each other, though no ^{56}Ni is synthesized and ejected during the pulsations. A high mass loss is predicted for stars with high zero age main sequence (ZAMS) mass in high metallicity environments. Therefore, the PISN and pulsational pair-instability events have been associated mainly with the population III stars in the early Universe. However, localized low metallicity environments in galaxies in the local Universe cannot be excluded (Scannapieco et al. 2005), and these events have been suggested to explain some of the observed super-luminous SNe, such as SN 2006gy as a pulsational pair-instability event (Woosley et al. 2007) and SN 2007bi as a PISN (Gal-Yam et al. 2009).

2.4 Thermonuclear supernovae

Although this thesis concentrates solely on CCSNe, thermonuclear SNe explosions of WD stars that are thought to give rise to SNe classified as Type Ia events, are also briefly discussed here for completeness. Phillips (1993) presented an empirical relation between the peak luminosity and the shape of the light curve of Type Ia SNe, that has made them excellent calibratable candles to measure cosmological distances, which led to the discovery of the accelerating expansion of the Universe (Riess et al. 1998; Perlmutter et al. 1999). For a recent review of the use of Type Ia SNe in cosmology, see Goobar & Leibundgut (2011).

Whereas CCSNe end the life cycles of massive stars, the Type Ia SNe originate from a thermonuclear explosion of a carbon-oxygen WD in a

binary system, when its mass exceeds the critical Chandrasekhar mass. Roughly 0.6 $M_\odot$ of radioactive ^{56}Ni is synthesized in a typical Type Ia explosion, however, for example in the extreme case of SNLS-03D3bb a ^{56}Ni mass of 1.3 $M_\odot$ was inferred, which is very close to the Chandrasekhar mass (Howell et al. 2006). The typical explosion energy of a Type Ia SN is $\sim 10^{51}$ erg, similar to normal iron-core-collapse SNe. The details of the thermonuclear explosion mechanism have, however, so far remained uncertain (for a review, see e.g. Hillebrandt & Niemeyer 2000). The commonly accepted WD explosion model is divided into two progenitor channels called the double degenerate and the single degenerate models. In the double degenerate model the SN explosion results from a merger of two WDs (e.g. Webbink 1984; Iben & Tutukov 1984). In the single generate model, however, the thermonuclear explosion results from the mass accretion from a non-degenerate main sequence, sub-giant, giant or helium star companion of the WD (e.g. Whelan & Iben 1973; Nomoto 1982), with the mass transferring either via Roche-lobe overflow or stellar wind capture. Observations and models have not been able to exclude either of the models, and it is also possible that Type Ia SNe are produced via both progenitor channels. Recently, based on pre-explosion images, Li et al. (2011c) ruled out luminous red giants and helium stars as a companion for the WD in the case of the nearby Type Ia SN 2011fe that exploded in the 'Pinwheel Galaxy' M 101.

2.5 Gamma-ray bursts

Gamma-ray bursts (GRBs) are highly energetic outbursts of γ-rays lasting up to a few seconds, often followed by a longer lasting afterglow emitting in a wide range of wavelengths, showing variety in luminosity and evolution. In a GRB the energy is released in a narrow beam and, if pointing towards the observer, it can be detected even at cosmological distances. Observationally the GRBs are divided into long lasting (> 2 sec) soft-spectrum and short lasting (≤ 2 sec) hard-spectrum GRBs (e.g. Gehrels et al. 2009). GRB progenitors, in particular in the case of short GRBs, have been suggested to be mergers in neutron star-neutron star or neutron star-black hole binary systems. However, it has been shown that at least some of the long GRBs are associated with an explosion of a massive star as a SN (see the review of GRBs and their connection to SNe by Woosley & Bloom 2006). The long GRBs with a CCSN connection have been explained with

a so-called collapsar model, where the iron-core of a massive star collapses into a black hole. An accretion disk of matter forms if the angular momentum is neither too high nor too low, and gravitational potential energy is converted into a collimated jet of matter and a beam of γ-rays in the polar regions blowing through the outer layers of the star with relativistic velocities (MacFadyen & Woosley 1999). In particular the observations have connected the GRBs to the so-called broad-line Type Ic SNe (Type Ic-BL), with the best examples being GRB 980425/SN 1998bw (Galama et al. 1998) and GRB 030329/SN 2003dh (Hjorth et al. 2003), which have shown very high kinetic energies of $\sim 10^{52}$ erg (Woosley & Bloom 2006). Statistical studies have also shown a correlation between the explosion sites of long GRBs and recent star formation (e.g. Fruchter et al. 2006), whereas this is not the case with the short GRBs (e.g. Gehrels et al. 2009).

Chapter 3

Core-collapse supernova types

In this chapter the main observational characteristics of different SN subclasses are summarized. The common way to classify SNe is based on their spectral lines. The sub-types are based on a historical convention with purely observational origin, not having necessarily any relevant physical connection. For a review of the subclass convention see Filippenko (1997). Alternative classification methods relying on the use of SN photometry and colours in common broad-band filters (e.g. Poznanski et al. 2002, 2007; Kuznetsova & Connolly 2007; Melinder et al. 2011) and in more specific narrow-band filters have been used and proposed, for example, for SN classifications in archive data, in high-redshift (high-z) surveys or in the new large scale wide-field surveys. Examples of low-resolution spectra of relatively young SNe of different subclasses observed with the Andalucia Faint Object Spectrograph and Camera (ALFOSC[1]) at the Nordic Optical Telescope[2] are presented in Fig. 3.1. These spectra include the Type Ia SNe 2009Q (Kankare et al. 2009), Type IIn SNe 2009kn (paper I) and 2008ip (Kankare et al. in prep.), Type IIP SN 2009az (unpublished), Type IIb SN 2011jg (Kankare et al. 2011) and Type Ic SN 2012ej (unpublished). It is worth noting that the spectra are by no means canonical represen-

[1]The data presented here were obtained with ALFOSC, which is provided by the Instituto de Astrofisica de Andalucia (IAA) under a joint agreement with the University of Copenhagen and NOTSA.

[2]Based on observations made with the Nordic Optical Telescope, operated on the island of La Palma jointly by Denmark, Finland, Iceland, Norway, and Sweden, in the Spanish Observatorio del Roque de los Muchachos of the Instituto de Astrofisica de Canarias.

tations of these subclasses, but rather examples of SNe falling into their respective categories.

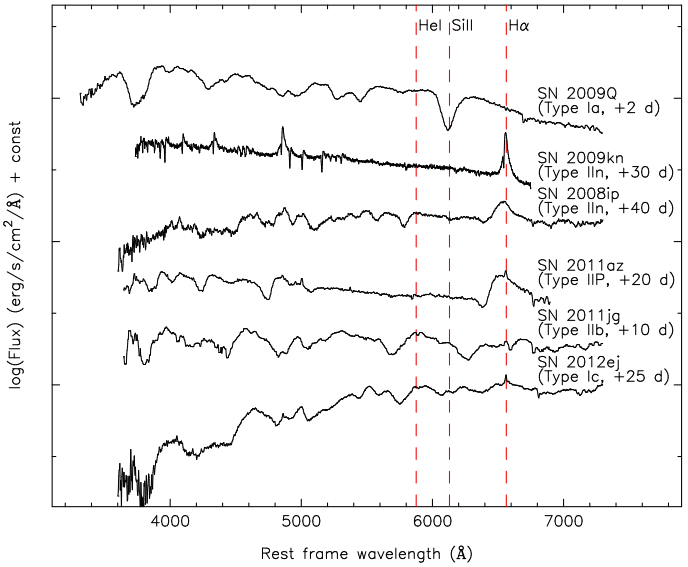

Figure 3.1: An example of optical spectra of different subtypes of SNe observed with the Nordic Optical Telescope. The spectra are wavelength corrected to the host galaxy rest frame and vertically shifted for clarity. SN types and approximate epochs relative to the optical peak are given in parenthesis. Most important lines (or lack of their presence) used for identifying SNe spectroscopically have been marked, i.e. Hα λ 6563, He I λ 5876 and the blueshifted Si II $\lambda\lambda$ 6347, 6371 doublet. Some spectra, i.e. SNe 2011az and 2012ej, may show in the plot very narrow hydrogen components, that are likely to have arisen from the host galaxy. Atmospheric features have not been removed.

3.1 Hydrogen-rich supernovae

All SNe that show hydrogen in their observed spectra are classified as Type II SNe and the most common subclass of these transients are the Type II plateau (Type IIP) SNe. The Type IIP and Type II linear (Type IIL)

SNe are practically indistinguishable, based on their spectral line profiles. However, whether or not the shape of the (optical) light curve is a plateau or linearly declining during the first ∼100 days classifies these Type II SNe into these two subtypes (e.g. Barbon et al. 1979; Doggett & Branch 1985).

Type IIP/L subtypes are the only SNe that are defined, not only by their spectroscopic appearance, but also by their photometric evolution. Recent results from the Caltech Core Collapse Project (CCCP), presented by Arcavi et al. (2012), indicate that the *R*-band light curves of the 'normal' Type II SNe may be divided into three distinctive subclasses without intermediate events: 'plateau', 'linearly declining' and 'rapidly declining'. The latter class consists solely of Type IIb events whose light curve decline is similar to that of Type Ib/c SNe, see Chapter 3.2.

The peculiar Type IIP SN 1987A was the first SN with a progenitor identified in pre-explosion images, which turned out to be a blue supergiant (BSG). However, the normal Type IIP SN progenitors are well established to be RSGs, both theoretically, and based on high-resolution progenitor observations, in particular using the *Hubble Space Telescope* (*HST*) data, with pre-explosion images of nearby ($\lesssim$20 Mpc) Type IIP events (Smartt et al. 2009). Based on both direct progenitor detections, and meaningful upper limits derived from pre-explosion images, the initial masses of the RSG progenitors of Type IIP SNe would range between ∼8 and 17 $M_{\odot}$, with a 2.4σ confidence (Smartt et al. 2009). As RSG stars with masses up to 25 $M_{\odot}$ are known to exist, this raises the question as to why higher mass RSG progenitors for Type IIP SNe have not been observed, which Smartt et al. (2009) calls the 'red supergiant problem'. In this work they found no strong evidence suggesting that the progenitor masses had been systematically underestimated due to extinction or that high mass RSG stars would explode as other Type II SNe. Instead, Smartt et al. (2009) suggested black hole formation without a luminous SN as an explanation for the lack of high mass RSG Type IIP progenitors. However, based on the relative CCSN rates from the Lick Observatory Supernova Survey (LOSS), Smith et al. (2011a) proposed instead that high mass RSG stars would evolve into other types of stars before core-collapse and would consequently explode as other Type II SNe. Recently Walmswell & Eldridge (2012) proposed circumstellar dust as the solution to the red supergiant problem. The dust forms close to the progenitor star in the RSG wind, relatively close in time before the core-collapse explosion and is destroyed by the initial UV flash from the shock breakout. This causes the dust to have a significant effect only on

the pre-explosion observations. The extinction thus decreases the brightness of the progenitors which, if not taken into account, will cause one to underestimate the progenitor masses. The model of Walmswell & Eldridge (2012) corrects the upper limit of RSG exploding as Type IIP SNe based on the progenitor observations to $\sim$21 $M_{\odot}$.

The RSG progenitors are thought to maintain most of their hydrogen envelope when the iron core collapses. During the plateau phase of a Type IIP SN, the internal energy deposited by the shock is released as photons diffuse out, and the hydrogen-rich outer envelope of the ejecta recombines. The optically thick photosphere dominates the observed luminosity and is receding in the expanding ejecta, maintaining a temperature of $\sim$6000 K and a fairly constant luminosity (see e.g. the review of SN explosions by Woosley & Weaver 1986). The plateau phase has a length of $\sim$100 days followed by a luminosity drop, and the light curve tail phase that is powered by radioactive decay of ^{56}Co. Contrarily, the Type IIL events are not as well understood. It is thought that they originate from similar progenitors as Type IIP SNe that have lost a significant fraction of their hydrogen envelope before collapse. If this process takes place via increased mass loss instead of mass transfer via binary interaction, this would indicate Type IIL SNe to have higher mass progenitors than those of Type IIP SNe (e.g. Smartt 2009).

3.2 Stripped-envelope supernovae

Type Ib/c SNe are defined by the lack of hydrogen in their observed spectra, and differentiated from Type Ia SNe by the absence of the blueshifted Si II $\lambda\lambda$ 6347, 6371 absorption line blend defining the Type Ia class. The Type Ib and Type Ic are further differentiated by their spectra: showing He I lines in the case of Type Ib SNe, and lacking these features in the case of Type Ic SNe. The strongest He I feature in the optical region is often the λ 5876 He I line. However, it is frequently difficult to clearly distinguish these two subtypes, so a Type Ib/c classification is also commonly used. It is also quite possible, that the two classes are not strictly separate, but form a continuous class of SNe.

The common model for Type Ib/c progenitors suggests that these SNe originate from WR stars that have lost their outer hydrogen envelope due to stellar winds, and in the case of Type Ic SNe, also their helium envelope,

prior to core-collapse. For example, in the review of WR stars by Crowther (2007) the nitrogen sequence WR stars (WN) are associated with Type Ib SN progenitors and carbon sequence WR stars (WC) with Type Ic SN progenitors. This model has also been supported recently, for example, by the statistical study of Leloudas et al. (2010) on the association to the host galaxy light of different types of WR stars and the explosion sites of Type Ib/c SNe. However, based on the lack of direct progenitor detections for Type Ib/c SNe in pre-explosion images, it seems likely that not all Type Ib/c progenitors are single massive WR stars (Smartt 2009). Instead, the outer envelope stripping of less massive stars in a binary interaction through Roche-lobe overflow, is an alternative progenitor channel for Type Ib/c SNe which have lost their outer hydrogen and possibly also helium shells (e.g. Podsiadlowski et al. 1992). Based on the relative CCSN rates from the LOSS sample, Smith et al. (2011a) concluded that the majority of Type Ib/c SNe would originate from progenitors in such a Roche-lobe overflow binary system.

Statistical studies have shown fairly clearly that Type Ib/c SNe are more centrally concentrated in their host galaxies than Type II SNe (e.g. Petrosian et al. 2005; Anderson & James 2009; Hakobyan et al. 2009). Particularly in disturbed galaxies Habergham et al. (2010, 2012) found a central excess of Type Ib/c SNe, which they associate with a top-heavy initial mass function (IMF) giving rise to a relatively higher fraction of very massive stars, especially in the central regions of these galaxies.

Anderson & James (2008) concluded that Type Ib/c SNe are more closely associated with H II regions than Type II SNe. Similar results were found recently also by Crowther (2013), emphasizing that the difference reflects the shorter life-times of more massive Type Ib/c progenitors, compared to H II regions and Type II SN progenitors. Similarly, based on the Sloan Digital Sky Survey (SDSS) data Kelly et al. (2008) found that Type Ib and II SN explosion sites generally followed the host galaxy g'-band light, whereas Type Ic SNe were found to be more closely associated with the brightest regions of the host galaxies. Anderson & James (2008) concluded that the explosion sites of Type Ic SNe trace Hα emission more closely than Type Ib SNe.

Transitional objects between Type II and Type Ib SNe that initially show hydrogen in their spectra similar to normal Type II SNe, but later evolve spectroscopically into Type Ib-like events are named as Type IIb SNe (Woosley et al. 1987; Filippenko 1988). As discussed in the previous

chapter, the light curve of these events often declines rapidly, resembling those of Type Ib/c SNe. Chevalier & Soderberg (2010) suggested dividing Type IIb SNe into compact (cIIb) and extended (eIIb) subgroups, observationally based on their radio luminosity. This subgrouping would also trace the mass of the progenitor hydrogen envelope, with cIIb SNe having the less massive hydrogen shells of $\lesssim 0.1$ $M_\odot$. A canonical example of the Type IIb group of SNe is the well-followed nearby SN 1993J in M 81, for which a K-type supergiant progenitor star in a binary system with a B-type supergiant companion was identified in pre-explosion images (Maund et al. 2004; Maund & Smartt 2009). More recently a Type IIb SN 2011dh was discovered in the nearby galaxy M 51, which started multiple observing campaigns and led to the identification of an F-type yellow supergiant progenitor candidate at the explosion site in the high-resolution pre-explosion images (Maund et al. 2011; Van Dyk et al. 2011). When the SN has faded enough, follow-up observations will show whether or not the progenitor candidate has disappeared, thus excluding this candidate detection from being dominated by a possible binary companion of the actual progenitor that exploded.

The common model for CCSN progenitors from low-mass to high-mass massive stars follows the sequence IIP $\rightarrow$ IIL $\rightarrow$ IIb $\rightarrow$ Ib $\rightarrow$ Ic. The border between Type II and Type Ib/c SN progenitor masses would be at $\sim 25 - 30$ $M_\odot$ (e.g. Heger et al. 2003; Eldridge & Tout 2004). However, placing the Type IIn SNe on this simple line of progenitor masses poses a difficult problem and I will discuss this heterogeneous group of SNe in more detail in Chapter 3.3.

3.3 Interacting supernovae

The narrow line Type II (Type IIn) subclass of SNe was first introduced by Schlegel (1990). The subclass is defined by narrow spectral lines [full width at half maximum (FWHM) $\lesssim 1000$ km s^{-1}] especially of hydrogen, superimposed commonly on an intermediate or a broad spectral line component (FWHM $\lesssim 10000$ km s^{-1}). This is considered as a sign of interaction between the SN ejecta and a dense CSM originating from a significant mass loss episode of the progenitor star (e.g. Chugai & Danziger 1994).

Although the narrow cores of the line profiles are the defining property of the Type IIn subclass, these SNe are otherwise the most heterogeneous

subclass. This heterogeneity is shown by the line profiles and their evolution, light curves and absolute magnitudes. However, in general the Type IIn SNe tend to be at the bright end of SNe, especially when compared to other Type II SNe (e.g. Richardson et al. 2002). This is one of the important features in distinguishing Type IIn SNe from so-called SN impostors, that can show narrow spectral lines resembling those of Type IIn SNe but can have peak luminosities comparable to those of, or lower than, low luminosity Type IIP SNe, i.e. $M_V = -14$ to -15 mag (Pastorello et al. 2006), see Chapter 3.4. Type IIn SNe are also relatively rare. The LOSS SN sample (Li et al. 2011a) suggests that Type IIn SNe form $\sim$7% of all CCSNe in their volume-limited (< 60 Mpc) sample, which is fairly consistent with the previous volume-limited (< 28 Mpc) estimate by Smartt et al. (2009). For the relative fractions of different CCSNe types from the LOSS sample, see Fig. 3.2.

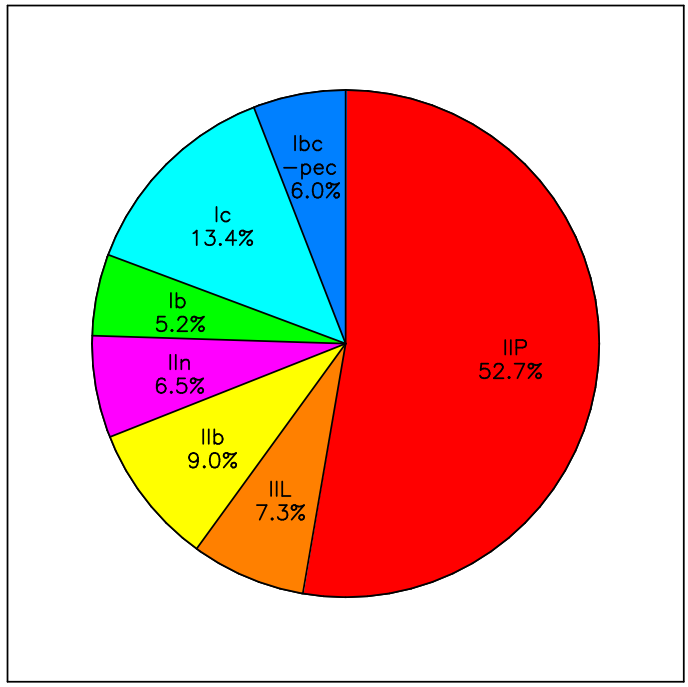

Figure 3.2: Pie chart of the fractions of CCSN types in a volume-limited Lick Observatory Supernova Survey SN sample from Li et al. (2011a).

So far the only direct progenitor detection inferred for a Type IIn SN from high-resolution pre-explosion images (and also confirmed by its disappearance) has been the progenitor of SN 2005gl, identified as an LBV star (Gal-Yam et al. 2007; Gal-Yam & Leonard 2009). An LBV progenitor has also been suggested for example for SN 2005gj, based on the high-resolution spectra of the SN having revealed a significant similarity of the CSM wind component with those of LBVs (Trundle et al. 2008). More recently it has been suggested that the third observed major outburst of the LBV SN 2009ip is a genuine SN explosion (see e.g. Pastorello et al. 2012) of the progenitor identified earlier as a 50−80 $M_\odot$ star. Furthermore, the analysis by Smith et al. (2011a) based on the observed fractions of CCSNe from the LOSS suggested that Type IIn SNe originate from the most massive stars. For discussion on the LBV progenitors for Type IIn SNe, see also Smartt (2009) and Dwarkadas (2011). However, these results challenge the current stellar evolution models, which predict that LBV stars should not directly explode as SNe, but instead evolve into WR stars and explode eventually as stripped envelope Type Ib/c SNe rather than Type IIn SNe (e.g. Langer et al. 1994; Maeder & Conti 1994).

On the other hand, relatively low mass RSG progenitors have also been suggested for some Type IIn SNe, such as in the case of SN 1988Z (Chugai & Danziger 1994). The pulsationally driven superwinds could increase the mass loss rate of RSGs to be up to $\sim 10^{-2}$ $M_\odot$ yr^{-1}, as proposed by Yoon & Cantiello (2010), leading to a significant loss of the hydrogen envelope. VY CMa is an example of a RSG in a superwind phase, for which Danchi et al. (1994) derived a mass-loss rate of $\sim 2{-}3{\times}10^{-4}$ $M_\odot$ yr^{-1}. VY CMa-like progenitors have been suggested for some relatively bright and slowly evolving Type IIn SNe such as SN 1988Z (Smith et al. 2009b), SN 1995N (Fransson et al. 2002) and SN 2005ip (Smith et al. 2009c).

In addition, some recent statistical studies (Anderson & James 2009; Kelly & Kirshner 2012) on the explosion sites of different types of CCSNe have found, that the Type IIn SN explosion sites do not differ significantly from those of Type IIP SNe. This seems to indicate similar progenitor masses for Type IIn as for the Type IIP SNe, that have been shown to originate from RSGs, i.e. low mass massive stars instead of very massive stars, such as LBVs. Recently, Anderson et al. (2012) increased the sample size from that of James & Anderson (2006) tracing the star formation with Hα and found, perhaps surprisingly, that Type IIn SNe follow less well the star formation than Type IIP SNe, indicating even lower average progenitor

masses for Type IIn than for Type IIP SNe.

The CSM interaction can be the dominating source of luminosity in Type IIn SNe for several hundreds of days after the explosion, and can also result in slowly declining light curves as, for example, in the case of SN 1988Z (Turatto et al. 1993). Another effect is that the spectra of Type IIn SNe do not necessarily enter the radioactive decay dominated nebular phase, observed typically in Type IIP SNe after the plateau phase ($\sim$100 days from the explosion). Furthermore, the typical forbidden nebular lines such as the [O I] $\lambda\lambda$ 6300, 6364 doublet and the Ca II] $\lambda\lambda$ 7291, 7325 doublet can be faint, or even absent, in the late spectra of Type IIn SNe, e.g. SN 1988Z (Stathakis & Sadler 1991) and SN 1998S (Fransson et al. 2005). A schematic diagram showing an idealized illustration of the basic components of a Type IIn SN in ejecta-CSM interaction is presented in Fig. 3.3

The range of types and masses of progenitors can be related to the afore-mentioned diversity of Type IIn SNe. As the Type IIn phenomenon is a result of CSM interaction, it is possible that the progenitor properties can differ within the Type IIn class of SNe. This heterogeneity of Type IIn SNe can be emphasized with a few examples of different kinds of narrow line SNe.

SNe sharing similarities to SN 1988Z (e.g. Turatto et al. 1993) are possibly the most typical Type IIn, SNe with multicomponent spectral line profiles and a slowly evolving light curve, as stated above. Other closely followed SNe with such properties include amongst others SN 1995N (Fransson et al. 2002), SN 2005ip (Smith et al. 2009c) and SN 2010jl (Smith et al. 2011b).

SN 1998S is a well followed Type IIn, to which other Type IIn SNe are often compared. Liu et al. (2000) concluded that the CSM envelope had expanded continuously in the form of a progenitor wind surrounding the progenitor star. However, two narrow components ($\sim$40$-$50 km s^{-1} and $\sim$400 km s^{-1}) were observed in the spectra of SN 1998S (e.g. Bowen et al. 2000; Fassia et al. 2001). Both Leonard et al. (2000) and Fassia et al. (2001) favour a model where the progenitor star had at least two episodes of asymmetric mass loss with a hiatus phase in between, explaining the observed changes in the line components. Both Liu et al. (2000) and Bowen et al. (2000) associated the progenitor with an RSG, and Pooley et al. (2002) derived a progenitor mass estimate of $\sim$15$-$20 M$_{\odot}$, based on elemental abundance analysis. Fassia et al. (2001) also suggested

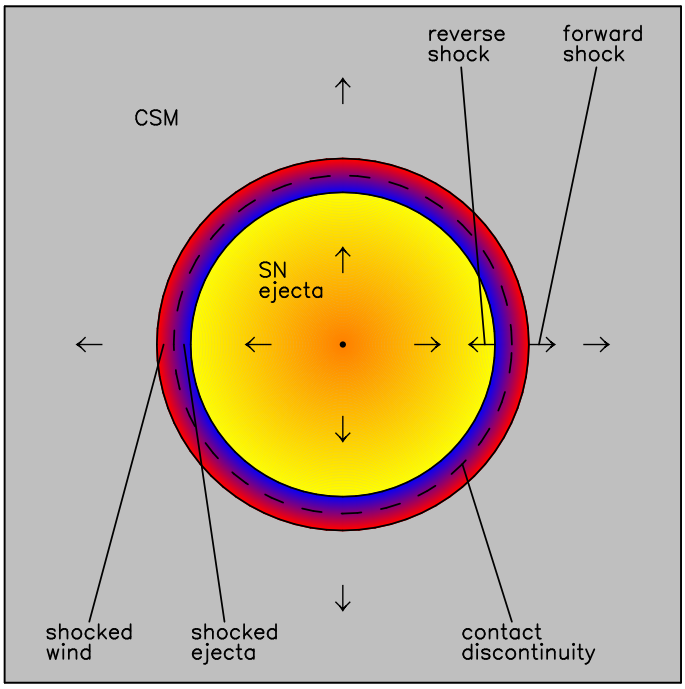

Figure 3.3: Schematic illustration of the components of the ejecta-CSM interaction (see Chevalier & Fransson 1994) displayed by Type IIn SNe (not to scale). The progenitor star is embedded in the CSM, typically rich in hydrogen, that can be, for example, in a form of a superwind or an outburst shell. The CSM component can be far more complex than illustrated here, including, for example, multi-component structure, density gradients or dense clumps. The initial UV/X-ray flash can photoionize the CSM and destroy some of the pre-existing dust, if present in the CSM. As the SN ejecta collides with the CSM a cool dense shell can form in the ejecta-CSM interface, bound by the shock waves (e.g. Chevalier & Fransson 1994). Typically, the ejecta can be expected to sweep up the slower CSM, unless the CSM component is exceptionally massive.

that the faster CSM wind component could originate from the BSG phase of the progenitor, where it had evolved from the RSG stage relatively shortly before the SN explosion. SN 1998S-like events seem to be common within the Type IIn subclass.

SN 1994aj and SN 1996L-like SNe (Benetti et al. 1998, 1999; Pastorello et al. 2011) can be considered as both Type IIn and Type IIL class events, with linearly declining light curves and line profiles with two main components: a narrow P-Cygni (absorption minimum at $\sim$700$-$900 km s^{-1}) component and a very broad emission component. Due to this profile structure they have also been dubbed as Type IId (II double) SNe (Benetti et al. 1999).

The early evolution of the SN 1994aj-like transients shares some similarities with SN 1994W-like Type IIn events. The nature of SN 1994W has been explained using very different models. Chugai et al. (2004) suggested that SN 1994W was a SN interacting with a dense $\sim$0.4 M$_{\odot}$ CSM shell ejected by the progenitor star $\sim$1.5 yr prior to the SN explosion. Dessart et al. (2009) concluded that the entire line profile can be explained as arising from a single optically thick region with internal electron scattering within the photosphere. As broad nebular lines, typical for a Type II SN in its late phases, were not observed in the tail phase spectra of SN 1994W, and the ^{56}Ni mass derived for SN 1994W was so low, Dessart et al. (2009) speculated on the possibility that the inner shell is not ejecta from a SN explosion, but a consecutive outburst of the massive progenitor star. The progenitor star would also survive the second outburst that would interact with the initial outer outburst shell. SN 2009kn, discussed in paper I, shares a significant similarity to SN 1994W. There has been great interest recently in SN 1994W-like events, with numerous publications appearing in the literature on SN 2011ht (Roming et al. 2012; Humphreys et al. 2012; Mauerhan et al. 2012).

SNe similar to SN 2002ic (Hamuy et al. 2003; Kotak et al. 2004; Benetti et al. 2006) and SN 2005gj (Aldering et al. 2006; Prieto et al. 2007; Trundle et al. 2008) have also been called Ia/IIn hybrid events, as they have been explained using two different scenarios: a Type Ia SN or a CCSN interacting with a CSM surrounding the progenitor. However, it seems that the majority of the studies favour the Type Ia scenario, the latest being the work done by Dilday et al. (2012) on PTF 11kx, based on very early spectra available for this event. Other transients of this very rare type of SNe include for example SN 1997cy (Turatto et al. 2000) and SN 2008J

(Taddia et al. 2012).

SN 2006jc-like (Foley et al. 2007; Pastorello et al. 2007, 2008) peculiar Type Ib SNe, that have also been labelled as Type Ibn SNe (Pastorello et al. 2007), show prominent and narrow He I lines. These events appear as a fairly normal Type Ib/c SNe, but show narrow lines of helium originating from a helium-rich CSM. In the case of SN 2006jc, a massive outburst that likely ejected the CSM was observed 2 years before the SN explosion, and has been explained as either an LBV-like outburst of the progenitor star or an outburst of an LBV companion of the progenitor (see e.g. Pastorello et al. 2007).

Extremely luminous CCSN events form a completely separate and very heterogeneous subclass of Type IIn/L SNe showing variety in their evolution. For a summary of such well followed events, see Gal-Yam (2012). Models for these kind of events include a strong interaction of the SN ejecta with the surrounding CSM. For SN 2006gy, in particular, several models have been suggested, e.g. pulsational pair-instability event by Woosley et al. (2007), compact LBV or WR star SN explosion surrounded by a $6-10$ $M_\odot$ clumpy CSM envelope by Agnoletto et al. (2009); or a very massive progenitor ($> 100 M_\odot$) surrounded by $\sim$20 $M_\odot$ CSM shell ejected in a η Carinae -like outburst by Smith et al. (2010a), see also Smith et al. (2007, 2008a) and Smith & McCray (2007).

3.4 Supernova impostors

Many of the SN impostors are thought to arise from LBV stars that undergo eruptive mass loss episodes without a core-collapse that would destroy the progenitor star. These outbursts have been associated with massive stars that are close to their Eddington luminosity $L_{\rm Edd}$, see Humphreys & Davidson (1994), but see also e.g. Dessart et al. (2010), Smith et al. (2011c) and Kochanek et al. (2012)

$$L_{\rm Edd} = \frac{4\pi c G M}{\kappa} \tag{3.1}$$

where c is the speed of light, G gravitational constant, M is the mass of the star and κ is the opacity coefficient. The physical mechanism of the outbursts is, however, not well understood (e.g. Smith et al. 2011c).

The light curves of SN impostors present a variety in peak magnitudes and evolutions. Besides being fainter than the real SN events, the decline from the luminosity peak of the SN impostors is typically faster and more sporadic than in the case of real SN events. In quiescence the LBVs can commonly show absolute magnitudes of roughly -8 to -10 mag (Pastorello et al. 2010) and outburst peak magnitudes of roughly -11 to -15 mag (Smith et al. 2011c; Kochanek et al. 2012), with some of them therefore reaching the luminosities of low-luminosity Type IIP SNe, such as SN 2005cs with $M_{R,\mathrm{plateau}} \approx -15$ (Pastorello et al. 2009). The expansion velocities of the ejected material indicated by the line profiles of SN impostors range from a few hundreds of km s^{-1} up to $\sim$1000 km s^{-1} (Smith et al. 2011c) thereby reaching the velocities shown by some of the Type IIn SNe in their spectra.

Some of these events have been clearly shown to be outburst events where the progenitor star survives, such as in the case of SN 2000ch (Wagner et al. 2004; Pastorello et al. 2010) and SN 2002kg/V37 (Weis & Bomans 2005; Maund et al. 2006) with observed multiple outbursts. For a review of SN impostors, see e.g. Smith et al. (2011c) and Kochanek et al. (2012).

The true nature of some of the intermediate luminosity optical transients peaking between bright novae and faint SNe has proven to be very controversial, such as the case of SN 2008S and the 2008 optical transient in NGC 300 (N300OT). Prieto et al. (2008) detected in the *Spitzer* archive 4.5, 5.8, 8.0 μm images the progenitor of SN 2008S, and found it to be consistent with an $\sim$10 M$_\odot$ AGB star heavily obscured by dust, and suggested that it exploded as an ECSN. Botticella et al. (2009) ruled out an LBV as the progenitor of SN 2008S, and instead found the transient to be consistent with an ECSN, based on the progenitor detection, weak explosion energy and the tail phase being consistent with the radioactive decay with a low ^{56}Ni mass. Similarly, an AGB progenitor was also favoured by Thompson et al. (2009). However, Smith et al. (2009a) and Berger et al. (2009) found spectral similarity between the yellow hypergiant IRC+10420 and both SN 2008S and N300OT, which led them to favour an LBV-like outburst scenario for the two events. Also both Bond et al. (2009) and Humphreys et al. (2011) suggested N300OT and SN 2008S to be luminous outbursts from non-LBV post-main sequence stars.

Chapter 4

Dust absorption & emission

Cosmic dust causes dimming of astronomical objects in all photometric and spectroscopic observations. In addition, and even more importantly, spectroscopic and multi-band photometric observations also suffer a relative extinction effect, where the photons in the shorter wavelengths are more heavily absorbed compared to the longer wavelengths, i.e. the light is reddened. Incorrect correction for the extinction effects can introduce errors in all the analyses based on the observations. Secondly, a large dust extinction can make an object unobservable. This leads to SNe not being discovered, even though their host galaxies were observed near the peak of the SN light curve, causing one of the most significant biasing errors in all SNR estimates. Therefore, in SNR studies accurate extinction estimates for the observed SNe and also corrections for the non-observed fraction of SNe are critically important.

4.1 Dust composition

Interstellar dust in the ISM is composed of grains with sizes ranging from ångströms to microns. Typically the dust grains are thought to have graphite and silicate composition, as these can explain the broad bumps in the extinction curve at $\sim$0.2 μm and $\sim$9.7 μm, respectively (see e.g. the review on interstellar dust by Draine 2003).

CCSNe have been suggested as significant sources of dust, in particular in the early Universe, however, direct observations have not supported the idea of CCSNe as major producers of dust (see e.g. Meikle et al. 2007; Szalai et al. 2011; and references therein). Other major sources of dust are thought to be winds of post-main-sequence giant stars, in particular AGB

stars (see e.g. Habing 1996; Höfner & Dorfi 1997). Also alternative sources of dust formation, such as accretion in molecular clouds (Gehrz 1989) and in quasar winds have been suggested (Elvis et al. 2002).

4.2 Dust extinction

The reddening of the light caused by dust extinction is given by the colour excess

$$E(B-V) = (B-V) - (B-V)_0 \tag{4.1}$$

where $(B-V)$ is the observed colour index and $(B-V)_0$ is the true colour of the source. The colour excess relates to extinction according to

$$R_V = \frac{A_V}{E(B-V)} \tag{4.2}$$

where a value $R_V = 3.1$ has been derived for the Galactic reddening. This value is also commonly used for other galaxies when a better estimate is lacking. However, different values for R_V have also been derived, such as $R_V = 4.05 \pm 0.80$ for the extinction law by Calzetti et al. (2000) for high SFR galaxies.

An optical depth τ of the medium results in an observed intensity I

$$I = I_0 e^{-\tau}. \tag{4.3}$$

where I_0 is the original intensity. Assuming pure absorption by the dust, the extinction in magnitudes is given by

$$A_\lambda = -2.5 \log(\frac{I_\lambda}{I_{0,\lambda}}), \tag{4.4}$$

i.e. the extinction A_λ in a given wavelength λ relates to the optical depth as

$$A_\lambda = -1.086\tau_\lambda. \tag{4.5}$$

During the past few decades various extinction laws have been derived, defining the dust reddening as a function of wavelength. A few most commonly used reddening laws are those derived by Rieke & Lebofsky (1985), Cardelli et al. (1989) and Calzetti et al. (2000). These extinction laws for the broad bands *UBVRIJHK* are shown in Fig. 4.1 and listed in Table 4.1 relative to the V-band.

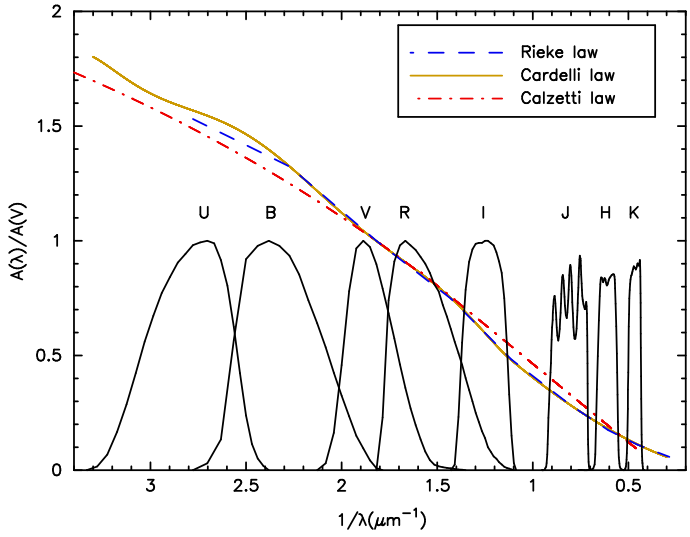

Figure 4.1: Rieke & Lebofsky (1985), Cardelli et al. (1989) and Calzetti et al. (2000) extinction laws in the optical and near-infrared region plotted respective to A_V. Johnsson-Cousins *UBVRI* (Bessell 1990) and The Two Micron All Sky Survey (2MASS) *JHK* (Cohen et al. 2003) filter functions are overplotted.

Typically the way to take into account the Galactic extinction at optical and near-infrared (near-IR) wavelengths has been the usage of the dust map by Schlegel et al. (1998) and more recently, recalibrated by Schlafly & Finkbeiner (2011). More problematic in many fields of extra

Table 4.1: Selection of commonly used extinction laws

band	λ_c (Å)	Rieke law A_λ/A_V	Cardelli law A_λ/A_V	Calzetti law A_λ/A_V
U	3600	1.531	1.569	1.488
B	4400	1.324	1.337	1.249
V	5500	1.000	1.000	1.000
R	7000	0.748	0.751	0.756
I	9000	0.482	0.479	0.539
J	12500	0.282	0.282	0.327
H	16500	0.175	0.190	0.195
K	22000	0.112	0.114	0.091

galactic astronomy is the estimation of extinction in targeted galaxies, for example in the observations of SNe. One of the most common ways to estimate the host galaxy extinction for a SN, has been a comparison of the equivalent width (EW) of the Na I D $\lambda\lambda$ 5890, 5896 absorption lines in the SN spectrum arising from the host galaxy, with those originating from the Galactic extinction (see Turatto et al. 2003). However, based on the examination of a large sample of Type Ia SN spectra, Poznanski et al. (2011) found large uncertainties in the method when low-resolution spectra are being used. In their subsequent work Poznanski et al. (2012) derived an empirical relation between the EW of the Na I D $\lambda\lambda$ 5890, 5896 absorption lines and the host galaxy extinction of

$$\log(E(B-V)) = 1.17 \times \mathrm{EW}(\mathrm{D}_1 + \mathrm{D}_2) - 1.85 \pm 0.08 \qquad (4.6)$$

to be used with spectra with high enough resolution.

Column density of the Na I line has also been used for extinction estimates. Fassia et al. (2000) converted these measurements from the spectra of SN 1998S to the column density of hydrogen, and derived the line-of-sight host galaxy extinction for the SN. Similarly, Mattila & Meikle (2001) used

the 21 cm radio observations of the hydrogen absorption to derive line-of-sight extinctions for the SN remnants in M 82. In both cases the relation between the hydrogen column density and the extinction by Bohlin et al. (1978) and Galactic gas-to-dust ratio were assumed.

Recently, Drout et al. (2011) presented a method to estimate the host galaxy extinction of Type Ib/c SNe, based on the $(V-R)$ colour on day 10 after the V-band peak. A comparison method to estimate the SN host galaxy extinction from light curves was used, for example, by Hendry et al. (2005) for the Type IIP SN 2003gd, using a χ^2 comparison of the observed optical light curves to those of SN 1999em.

Comparison of the observed SN light curves to reference light curves is a very useful method, especially in the absence of spectra, for deriving host galaxy extinctions and explosion epochs. The comparison can be carried out using as a reference either light curves of well followed SNe or template light curves derived for a group of SNe. The method can be generalized, for example, in the following way for CCSNe assuming prior knowledge of the distance to the SN. Three parameters can be derived simultaneously: the time t from the normalized zero epoch of the template, the V-band extinction A_V of the host galaxy, and a constant shift of the magnitudes C describing the intrinsic difference between the absolute brightness of the SN and the reference. The C is a constant for all the bands and epochs, assuming the same intrinsic colours, in a given fit

$$M_\lambda(A_V, t, C) = \\ m_\lambda(t_0 + t) - 5\log\left(\frac{d}{10\mathrm{pc}}\right) - \left(\frac{A_\lambda}{A_V}\right)^{\mathrm{Gal}} A_V^{\mathrm{Gal}} - \left(\frac{A_\lambda}{A_V}\right) A_V - C. \quad (4.7)$$

Here M_λ is the absolute magnitude, m_λ the observed magnitude, t_0 the data epoch respective to the discovery date, d the luminosity distance in parsecs, and A_λ/A_V the extinction law. The template fitting can be carried out by searching for the lowest χ^2 value within the parameter space for the variables A_V, t and C, when comparing the observed data points converted into absolute magnitudes M and the template light curves M_T

$$\chi^2(A_V, t, C) = \sum_{i=1}^{n} \left(\frac{M_i(A_V, t, C) - M_T(A_V, t, C)}{m_i^{\rm err}} \right)^2, \qquad (4.8)$$

where $m^{\rm err}$ is the error of photometry for the given data point.

As noted in Chapter 3, broad-band photometry has been used more commonly to derive likely types of SNe (e.g. Poznanski et al. 2002, 2007; Kuznetsova & Connolly 2007; Melinder et al. 2011). Usually these photometric classification methods rely on template comparison using the Bayesian probability approach. However, the goal of these studies has usually been to identify the Type Ia SNe in the candidate sample, though the basic principle is expandable to be used for CCSN subtypes as, for example, in Melinder et al. (2011). For completeness, it can also be mentioned, that for Type Ia SNe a so-called multicolor light curve shape (MLCS) method (Riess et al. 1996) is often used to derive host galaxy extinctions.

In the above-mentioned work by Hendry et al. (2005) additional estimates of line-of-sight host galaxy extinction were also obtained by measuring reddening towards nearby stars and H II regions. Hydrogen line ratios derived from the SN spectra have also been used to estimate host galaxy extinction (e.g. Maiolino et al. 2002), which can be a useful method if intrinsic line ratios can be assumed, based on, for example, case B recombination (Osterbrock & Ferland 2006).

4.3 Dust emission in supernovae

An excess of IR luminosity compared to the intrinsic SN emission, can arise from either pre-existing dust in the CSM or newly formed dust in the SN ejecta and/or the CSM (see e.g. Gerardy et al. 2002). In the case of pre-existing dust, it is expected that the initial UV/X-ray flash will evaporate dust close to the progenitor. However, the surviving pre-existing dust outside the evaporation radius, can give rise to an IR echo (e.g. Dwek 1983; Graham et al. 1983) where the dust absorbs the SN peak luminosity, heating up the dust, which then re-radiates the energy at IR wavelengths. Alternatively, the near-IR excess can be powered by the kinetic energy of the ejecta transfered in the collision of the ejecta with the pre-existing CSM gas. If new dust is condensed, this can take place either in the freely expanding ejecta (e.g. Lucy et al. 1989) or in a cool dense shell (CDS) (e.g.

Pozzo et al. 2004) between the forward and the reverse shocks. The IR excess from the newly formed dust can be powered by radioactivity or the ejecta-CSM interaction. In the case of new dust forming in the ejecta or CDS, the dust extinction increases and causes the SN optical luminosity to decrease and the emission line profiles to shift bluewards. In particular, detecting the latter effect can be considered as strong evidence of new dust formation (Lucy et al. 1989).

IR excess has been observed in several Type II SNe, see e.g. Fox et al. (2011; and references therein) for a list of 30 such events. A near-IR excess has also been observed in the case of the controversial Type IIn event SN 2008S (Botticella et al. 2009), as well as in the SN impostor, the 2009 outburst of an optical transient in UGC 2773 (Smith et al. 2010b; Foley et al. 2011).

Unlike with the Type II SNe, with Type Ib/c SNe emission from pre-existing or newly formed dust has not been generally observed (Taubenberger et al. 2009; and references therein); the only exceptions being the Type Ib SNe 1982E and 1982R (Graham & Meikle 1986), the Type Ib SN 1990I (Elmhamdi et al. 2004) and the peculiar Type Ibn SN 2006jc (e.g. Mattila et al. 2008; Smith et al. 2008b).

Chapter 5

Supernova searches & rates

A few particular steps in the development of new technologies has increased significantly the number of SNe discovered since the invention of the telescope. A few decades ago, in the mid-1990s, progress was made by the adoption of charge-coupled device (CCD) cameras by professional and amateur astronomers, which led to significantly more new SNe being discovered. The most recent such leap in progress has been the new large scale sky surveys for transient objects, such as the Palomar Transient Factory (PTF), the Panoramic Survey Telescope and Rapid Response System (Pan-STARRS) and the planned Large Synoptic Survey Telescope (LSST).

Based on SN discoveries SNRs can be derived. The SNR simply represents the number of SNe that explode within a defined time period and galaxy sample, given either as a function of galaxy luminosity or volume, in units of SN (100 yr)$^{-1}$ (10^{10} $L_{B,\odot}$)$^{-1}$ or SN yr^{-1} Mpc^{-3}, respectively. However, the cosmic SNR is expected to evolve significantly as a function of redshift. As massive stars have a short life cycle that ends in a CCSN explosion, the rate of these SNe provides a tool to measure the ongoing SFR (e.g. Dahlén & Fransson 1999), which is independent of other factors such as the usage of the galaxy luminosity as a tracer of star formation. If measured over the complete redshift range, this would provide the complete cosmic star formation history of the Universe.

The relation between the expected CCSN rate $\nu_{\rm SN}$ and the SFR depends on the mass range of the CCSN progenitors and on the IMF $\phi(m)$

$$\nu_{\rm SN} = \frac{\int_{8M_\odot}^{50M_\odot} \phi(m)\mathrm{d}m}{\int_{0.1\ M_\odot}^{125M_\odot} m\phi(m)\mathrm{d}m} \times \mathrm{SFR}. \tag{5.1}$$

Assuming the Salpeter IMF (Salpeter 1955) for stars between 0.1 and 125 $M_\odot$ and a mass range of CCSN progenitors of 8 to 50 $M_\odot$ yields a relation $\nu_{SN} = 0.0070 \times SFR$.

5.1 Core-collapse supernova rates in the local Universe

Not surprisingly several statistical studies on CCSNe have been published exploring, for example, the distribution of CCSNe in different types of host galaxies (e.g. Petrosian et al. 2005; Leaman et al. 2011) and the radial distribution of CCSNe in their host galaxies (e.g. Petrosian et al. 2005; Anderson & James 2009; Hakobyan et al. 2009; Habergham et al. 2010, 2012). Similarly, the association of CCSNe to various components of their host galaxies has been studied statistically, e.g. the association of CCSNe with the host galaxy spiral arms (e.g. Petrosian et al. 2005), the association of CCSNe with the host galaxy luminosity distribution (e.g. Kelly et al. 2008; Kelly & Kirshner 2012), the association of CCSNe with the host galaxy stellar populations (e.g. Leloudas et al. 2010) and the association of CCSNe with the H II regions (e.g. Petrosian et al. 2005; Anderson & James 2008; Crowther 2013). Also the relative frequencies of different CCSN types (e.g. Prantzos & Boissier 2003; Arcavi et al. 2010; Habergham et al. 2010, 2012; Li et al. 2011a) have been derived, using various galaxy samples. All these studies rely on certain assumptions on the completeness of the used SN sample and require sufficient statistics to derive meaningful conclusions. However, it is the SNR studies that pose the most constraining requirements for a complete volume-limited SN sample.

One of the first works on CCSN rates with relatively large data statistics was the one by Cappellaro et al. (1999), making use of the SNe that had been discovered at the time, combined with the results of the visual SN search carried out by Robert Evans for close to two decades (Evans 1997). The derived rate should, however, be considered as a robust lower limit for the SNRs and SFRs in the local Universe.

In Smartt et al. (2009) the local CCSN rate was derived, based on all the discovered SNe within 28 Mpc during a 10.5 yr period. Of course this sample includes significant observational biases as, for example, both amateur and professional SN surveys are more inclined to follow face-on galaxies than highly inclined galaxies. Similarly, a significant fraction of intrinsically

faint SNe and highly extinguished SNe are certainly being missed in all the current SN surveys. The question remains, as to how large these fractions really are. Therefore, as with the rates derived by Cappellaro et al. (1999), the rates reported by Smartt et al. (2009) should be considered as well-defined lower limits for the true local core-collapse SNR and SFR.

In the work by Botticella et al. (2012) the volume of the CCSN sample was further decreased by deriving the CCSN rate just within 11 Mpc, based on SNe discovered during the last 13 years. In addition, they carried out a study to compare different tracers of the SFR, e.g. far-UV and Hα luminosity, with the observed CCSN rate, to verify the principle of using CCSNe as a tracer of on-going star formation. They found that the SFR indicated by the far-UV luminosity agreed well with the CCSN rate, whereas the often used Hα luminosity underestimated it roughly by a factor of two.

The best volume-limited CCSN rates so far in the local Universe have been derived from the fantastic data set obtained in the Lick Observatory Supernova Search (LOSS) conducted with the 0.76 metre robotic Katzman Automatic Imaging Telescope (KAIT; Filippenko et al. 2001) and reported in Leaman et al. (2011) and Li et al. (2011a,b). The survey was conducted with unfiltered observations, corresponding closest to the R-band of the Johnson-Cousins filter system. In Li et al. (2011b) the CCSN rates were derived, based on a sample of 440 CCSNe that were discovered at any time during the survey, in a sample of 10121 galaxies dubbed as the 'optimal' galaxy sample. The sample excluded early type E/S0 galaxies and small (major axis < 1.0 arcmin) galaxies, as well as highly inclined galaxies ($i > 75^\circ$) due to the possible extinction effects. Li et al. (2011b) found that the smaller galaxies have relatively higher SNRs, and showed that it is necessary to describe the rates with a so-called rate-size relation, including galaxy size as the secondary parameter in addition to such factors as the galaxy colour or the Hubble type.

5.2 Image subtraction methods

The comparison of new images with an older reference image for potential transient targets is a crucial method in SN searches. The simplest way to do this is by eye. However, more quantitative methods include image subtraction between the two images obtained in different epochs, and some variation of this method is used in most of the professional SN searches.

One of the most commonly used algorithms in the image subtraction is the ISIS 2.2 Optimal Image Subtraction (OIS) software presented in Alard & Lupton (1998) and Alard (2000), originally developed for the purpose of accurate photometry of variations detected in microlensing surveys. The method is based on point spread function (PSF) matching image subtraction, and is conducted on a pair of images that are first aligned spatially. As discussed by Israel et al. (2007) a slight misalignment of the images can be compensated in the OIS method by spatial variety of the convolution kernel, however, for best results the images should be aligned as well as possible. Both point and extended sources for these selected kernel regions in the image are accepted by the algorithm, with preference for a high signal-to-noise ratio. For the aligned images, ISIS 2.2 matches the PSF, the flux level and the variation of the background levels of the better seeing image to the worse seeing image, using a convolution kernel. The optimal kernel is found in the method by deriving a least-squares solution, comparing all the pixels between a pair of images (Alard & Lupton 1998).

As noted, for example, by Melinder et al. (2008) a very small kernel size ($<$ FWHM) will likely cause the image subtraction to fail, whereas increasing the kernel size will increase the noise in the subtracted image. In general the image subtraction process is expected to increase the noise at least by a factor of $\sqrt{2}$ (Alard & Lupton 1998). Typically, the residuals and the noise from the subtracted host galaxy are the dominating factors in the quality of the SN sites in the subtracted images, and the modification of the polynomial orders and sigmas of the Gaussian functions have little effect on the OIS method, as found by Melinder et al. (2008). Contrarily, the modification of the polynomial orders of the kernel spatial variation and the background fitting model can be very useful for subtractions with complex convolution solutions or background gradients. Subsequent attempts to improve image subtraction algorithms have also appeared in the literature (e.g. Yuan & Akerlof 2008; Bramich 2008), often based on the basic method of convolving the images implemented in ISIS 2.2.

5.3 Luminous infrared galaxies

The IR luminosity of some galaxies can be considered as an indicator of their SFR. This is particularly true for high SFR galaxies, such as the luminous (10^{11} $L_\odot < L_{IR} < 10^{12}$ $L_\odot$) infrared galaxies (LIRGs) and ultraluminous

($L_{IR} > 10^{12}$ $L_\odot$) infrared galaxies (ULIRGs). For a review of U/LIRGs see Sanders & Mirabel (1996). U/LIRGs are often merger events of two or more galaxies, where the interaction enhances the star formation, especially in the central regions where the gas is falling. Therefore, the morphology of U/LIRGs can differ significantly from normal spiral galaxies with symmetrical disk, spiral arm and bar structure, as U/LIRGs can display a variety of multiple and extended nuclei, star formation rings surrounding the core, bright H II regions, super star clusters, warping, tidal tails and overall irregularity in the shape (e.g. Scoville et al. 2000). Gemini-North adaptive optics K-band images of the eight LIRGs followed in the search for highly obscured CCSNe in LIRGs (see papers II & III), are shown as an example in Fig. 5.1. Besides high SFRs, the large IR luminosity can also be partially powered or even dominated by an active galactic nucleus, and separating these two power sources can be problematic (e.g. Alonso-Herrero et al. 2012). Though the fraction of galaxies with high SFRs in the local Universe is small, at cosmological distances the LIRGs and ULIRGs become more important, and eventually at high redshift $z \gtrsim 0.7$ they start to dominate the SFR (Le Floc'h et al. 2005; Magnelli et al. 2009, 2011).

In fact, with proper calibration CCSNe can provide a valuable new tool to measure SFRs via SNR measurements, independent from the galaxy luminosity based methods (e.g. Dahlén & Fransson 1999). Closely related to this, and to any SNR study in U/LIRGs, is the high host galaxy extinction that prevents most SN surveys from discovering SNe in such galaxies. Discoveries of CCSNe in nearby U/LIRGs can also be used to map the U/LIRG extinctions if a large enough number of SNe with derived extinctions are available. Finally, the CCSN population itself in U/LIRGs is a question of interest. A recent study by Anderson et al. (2011) suggested that the CCSN population of the LIRG system Arp 299 has a larger fraction of stripped envelope Type Ib/c and Type IIb SNe than normal spiral galaxies, which they associated either with a young age of the starburst and/or a different IMF producing a larger fraction of higher mass stars compared to normal spiral galaxies. They also concluded that the stripped envelope SNe discovered in Arp 299 are more centrally concentrated than Type II SNe, however, this has also been well established for normal spiral galaxies, see Chapter 3.2. Unfortunately, these kind of systematic studies of CCSN populations in U/LIRGs have so far been problematic, due to the low number of SNe discovered in optical/near-IR searches. Even the statistical study of Anderson et al. (2011) suffers from this problem, as it

was only based on seven CCSNe.

Arp 299 is considered a prototypical LIRG due to its high IR luminosity $\log L_{IR} = 11.88$ $L_\odot$ and the merger morphology consisting of two main components: IC 694 (Arp 299-A) and NGC 3690 (Arp 299-B). Due to its small distance of only ∼50 Mpc, it is one of the closest LIRGs and it has been the subject of extensive studies. So far seven SNe have been discovered in Arp 299 in optical/near-IR, and the CCSN rate for Arp 299 can be estimated to be ∼2 SNe yr^{-1}, based on IR luminosity. Most of the star formation and the SN explosions are concentrated in the nuclear regions of the two component galaxies, which has been well established by very-long-baseline interferometry (VLBI) radio observations, with the advantage of milliarcsecond resolution. These observations have revealed numerous compact radio sources, identified as radio SNe and SN remnants within the ∼100−150 pc and ∼30 pc central regions of the A and B1 nuclei of Arp 299, respectively (Pérez-Torres et al. 2009; Ulvestad 2009; Bondi et al. 2012).

Similar radio observations have also been carried out on the prototypical ULIRG Arp 220 (Lonsdale et al. 2006; Parra et al. 2007; Batejat et al. 2011) revealing a rich radio SN and SN remnant population within ∼200 pc within both of the two nuclei. Based on the VLBI observations Lonsdale et al. (2006) derived an estimated CCSN rate of 4±2 SNe yr^{-1} for Arp 220. Recently, Herrero-Illana et al. (2012) showed that the nuclear distribution of SNe detected in radio in starburst galaxy M 82, LIRG IC 694 and ULIRG Arp 220 follows exponential nuclear disks with scale lengths of ∼20−30 pc for the U/LIRGs and ∼140 pc for M 82.

As the IR bright galaxies with higher SFRs are expected to have high dust extinctions, carrying out an SN search at near-IR wavelengths has a clear advantage over optical wavebands, as the extinction is reduced by a factor ∼10. For example Grossan et al. (1999) conducted one of the first K-band SN searches using a sample of 177 IR bright starburst (and some normal) galaxies within 25 Mpc. Similarly, Mannucci et al. (2003) conducted a K'-band monitoring campaign of 46 LIRGs within ∼200 Mpc. A Ks-band SN search in a sample of 40 starburst galaxies within 45 Mpc was carried out by Mattila & Meikle (2001) and Mattila et al. (2004).

However, typically these searches that rely on natural seeing have fallen short on the expected number of SNe detected, based on IR luminosity. In fact, in the searches for SNe in high SFR galaxies the use of near-IR observing is not sufficient. High spatial resolution is also required, as star formation in such galaxies is concentrated in the nuclear regions (e.g. Soifer et al.

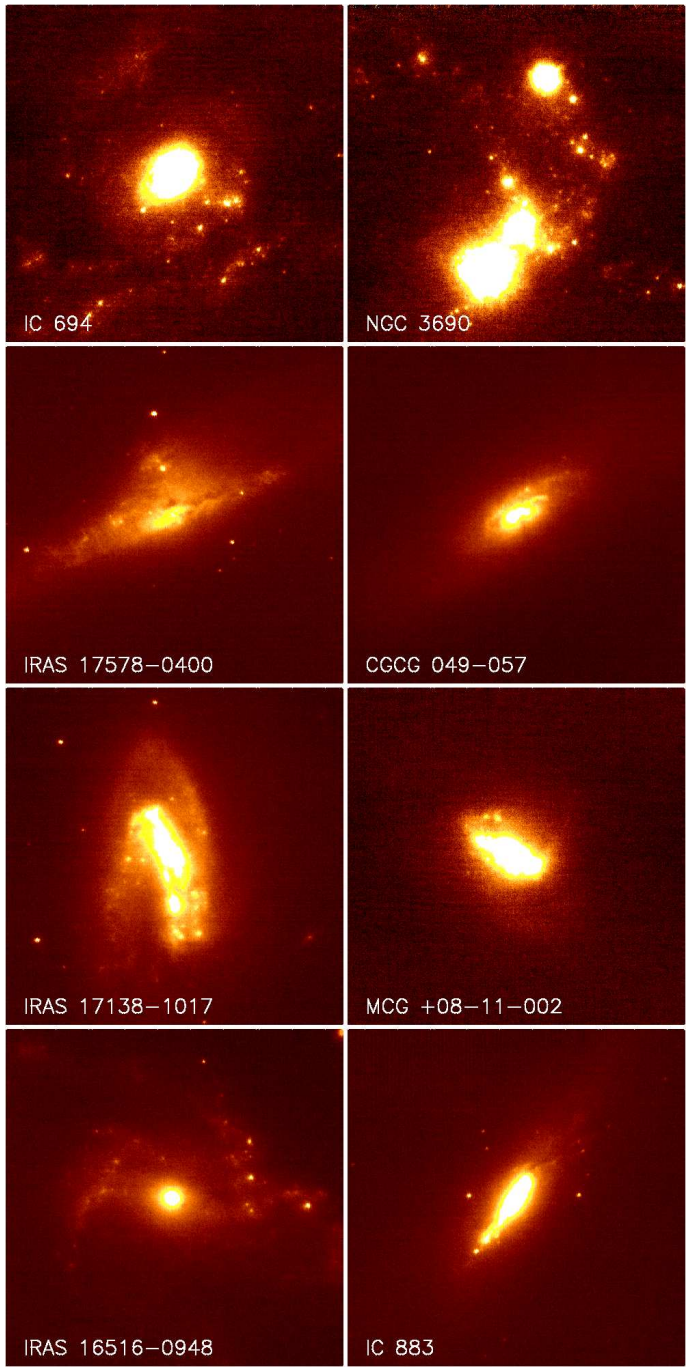

Figure 5.1: $15'' \times 15''$ Gemini-North ALTAIR/NIRI adaptive optics K-band images of a sample of nearby luminous infrared galaxies.

2001). Earth's turbulent atmosphere blurs the images obtained by telescopes. This effect can be compensated by building the telescopes on high altitude mountain sites with relatively stable atmospheric conditions, however, to truly achieve the telescopes diffraction limited seeing conditions, the use of ground-based adaptive optics (AO) or space-based telescopes such as the *HST* is required. AO imaging is based on the use of a wavefront sensor that monitors the variations on the natural or artificial laser guide stars (LGSs) to calculate high-order corrections to a deformable mirror on the light path, and to compensate for these distortions in real time, hundreds of times in a second (for a review on AO see Davies & Kasper 2012). In a pilot study conducted by Mattila et al. (2007) with the Nasmyth Adaptive Optics System Near-Infrared Imager and Spectrograph NAOS-CONICA (NaCo) (Lenzen et al. 2003; Rousset et al. 2003) on the ESO Very Large Telescope (VLT) using natural guide star (NGS) AO, SN 2004ip was discovered within the nuclear region of a LIRG IRAS 18293-3413 and a host galaxy extinction in the range of $A_V = 5 - 40$ mag was estimated, based on the K-band light curve.

5.4 Core-collapse supernova rates in the high-z Universe

Local SNR studies have relied mainly on heterogeneous sets of available data within a given volume, including SNe discovered in searches carried out by a range of both amateur and professional astronomers without properly documented details on the searches. However, the current generation telescopes have enabled deep and systematic SN searches to be carried out in the increased volume of the higher redshift Universe, to derive estimates for the SNRs. In particular, a lot of work has been done in the field of intermediate and high-z Type Ia SNRs (e.g. Dahlen et al. 2008; Dilday et al. 2010; Rodney & Tonry 2010; Graur et al. 2011), and recently intermediate and high-z CCSN rates have also become available.

In Dahlen et al. (2004) CCSN rates at $\langle z \rangle = 0.3$ and 0.7 were derived. These rates were based on 17 CCSNe discovered with the *HST*. Their search was done in the z-band (F850LP), with follow-up in V and i-bands (F606W, F775W). The model of Hatano et al. (1998) was used in their work for the extinction correction. The CCSN rates reported in Dahlen et al. (2004) were preliminary results, with the full data set being

reported in Dahlen et al. (2012), with derived rates at $\langle z \rangle = 0.39$, 0.73 and 1.11, based on 45 CCSNe using a more realistic correction for host galaxy extinctions (see paper V).

The CCSN rate from the Southern inTermediate Redshift ESO Supernova Search (STRESS) was derived in Botticella et al. (2008) at $\langle z \rangle = 0.21$. Their search was carried out with the MPG/ESO 2.2 metre telescope in V and R-bands with additional observations in B and I. Their target fields included 43283 galaxies with known photometric redshifts, and during the six year survey they discovered 16 confirmed CCSNe with 64 additional candidates. For the extinction correction Botticella et al. (2008) used a slightly modified version of the CCSN host galaxy extinction model of Riello & Patat (2005).

Bazin et al. (2009) derived a CCSN rate relative to the Type Ia SN rate at $\langle z \rangle = 0.3$. They used a sample of 117 CCSN candidates from a three year period of *g'*, *r'*, *i'* and *z'*-band data obtained in the Supernova Legacy Survey (SNLS) carried out at the Canada-France-Hawaii Telescope (CFHT). For the host galaxy extinction correction they used the model of Hatano et al. (1998).

Graur et al. (2011) concentrated on Type Ia SNe in their high-z rate study carried out with the Subaru telescope, however, they also derived a CCSN rate at $\langle z \rangle = 0.66$. Their observations were obtained in R, *i'* and *z'*-bands in four epochs over three years. For the extinction correction they adopted the missing fractions of SNe as derived by Mannucci et al. (2007), attempting to correct in particular for higher extinctions in starbursting galaxies. This is especially important at higher redshifts with increased fractions of starbursting LIRGs and ULIRGs as CCSN hosts instead of normal spiral galaxies, compared to the local Universe, as discussed in Chapter 5.3. In the local Universe Mannucci et al. (2007) assumed that only 5−10 % of the CCSN are missed by optical searches, with the missing SN fraction $f(\mathrm{CCSN})$ increasing linearly as a function of redshift, due to an increasing population of CCSNe in U/LIRGs: $f(\mathrm{CCSN}) = 0.05 + 0.28z$ % within $z \leq 2$. Their optical missing fraction for LIRGs (∼90 % in the local Universe) is the one estimated from the survey data summarized in Mannucci et al. (2003). This missing fraction is only based on three CCSNe, that were discovered in a sample of 46 LIRGs within 200 Mpc in a 2.2 μm SN search carried out with ground-based telescopes over a period of two years. From the three CCSNe, one was also independently discovered by an optical survey. Based on these results and assumed fractions of

CCSNe in the nuclear and outer regions of LIRGs, Mannucci et al. (2003) derived an estimate for the CCSN rate in LIRGs, from which an optical missing fraction was inferred for Mannucci et al. (2007).

The CCSN rate from the Stockholm VIMOS Supernova Survey (SVISS) was derived in Melinder et al. (2012) for both $\langle z \rangle = 0.39$ and 0.73. Their sample consisted of nine classified CCSNe discovered during four years in a survey carried out with the VLT in R and I-bands. The extinction corrections adopted for the rates were from paper V.

For a plot on CCSN rates as a function of redshift derived recently in the literature, see Fig. 5.2.

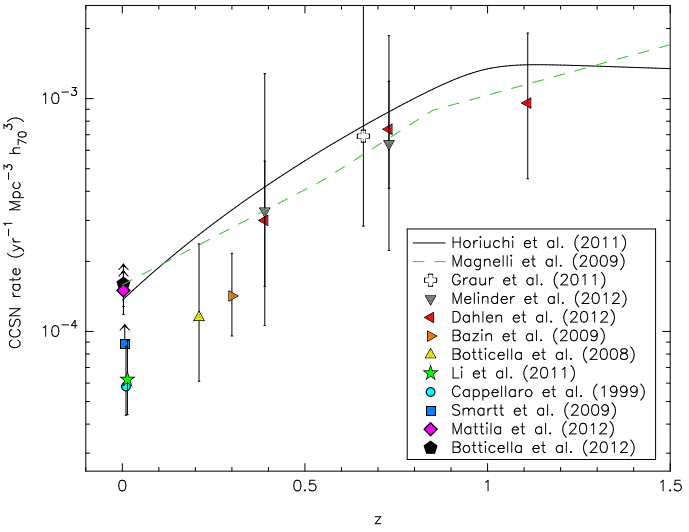

Figure 5.2: CCSN rates from the literature. The derived CCSN rate of Dahlen et al. (2012) and SFR curves of Magnelli et al. (2009) and Horiuchi et al. (2011) are shown as presented in Dahlen et al. (2012). Other values have been obtained from Melinder et al. (2012).

Optical SN searches are highly biased by dust extinction in SN host galaxies, preventing highly obscured SNe being discovered both in high-z and also in the local Universe. Horiuchi et al. (2011) suggested in their recent study based on the CCSN rates available at the time, that the observed cosmic CCSN rate is roughly a factor of two lower than the predicted SFR of massive stars, a problem which they dub as the 'supernova rate prob-

lem'. In their work they discuss various factors that can contribute to this discrepancy, such as extinction corrections for SNRs, errors in the derived SFRs and the contribution of faint CCSNe, stating the most likely explanation to be populations of CCSNe that are intrinsically faint or highly obscured.

Chapter 6

Summary of the articles

The publications included in this thesis do not concentrate on one specific area of CCSN research, but instead study how dense and dusty environments affect these transients as they are observed. The group of authors are referred to in the following as 'we'. My contributions to the publications are summarized at the end of each section.

6.1 Paper I

In Paper I an extensive data set of SN 2009kn is presented, covering the photometric and spectroscopic evolution of the transient in optical and near-IR wavelengths during the first ∼1.5 yr since the discovery. Spectroscopically SN 2009kn has been classified as a Type IIn event, based on narrow Balmer lines (FWHM $\sim$ 1000 km s^{-1}) with prominent P-Cygni profiles during the plateau phase. However, the light curve plateau resembles that of a normal Type IIP SN. SN 2009kn was shown to be a close twin of the exceptional Type IIn event SN 1994W both spectroscopically and photometrically. The major difference between the two transients is the post-plateau light curve tail phase, which in the case of SN 2009kn seems to follow the theoretical radioactive decay slope of ^{56}Co. This supports the SN nature of SN 2009kn with inferred ^{56}Ni mass of 0.023 M$_{\odot}$.

Similar Hα line profile components were identified in the spectra of SN 2009kn that are evident in the spectra of SN 1994W. The luminosity of the broad (FWHM $\sim$ 3000 km s^{-1}) component was found to follow the luminosity of the narrow P-Cygni component during the plateau phase, i.e. $L_{\rm broad}(t) \propto L_{\rm P-Cygni}(t)$. It was concluded that the broad component is arising from internal electron scattering in the photosphere, based on the

above mentioned luminosity relation, the symmetry of the broad component, the fact that it disappears after the light-curve drop and the absence of broad lines without an overlapping narrow component. This follows the model of Dessart et al. (2009) for explaining the spectral line profiles of SN 1994W.

Dessart et al. (2009) also suggested a scenario of two consecutive outbursts, which did not destroy the progenitor star, for the origin of SN 1994W. Interaction of the outburst shells would explain the observed high luminosity, which is however, also consistent with ejecta-CSM interaction of a CCSN. We could not exclude the multiple outburst scenario for the origin of SN 2009kn. However, the light curve seems to follow the radioactive decay of ^{56}Co in the tail phase. At the same time the luminosity during the light curve tail phase is dominated by narrow line emission in the absence of continuum and broader nebular ejecta lines. If SN 2009kn was an SN, this suggests that the narrow line component is arising from low velocity ejecta. The low inferred ^{56}Ni mass, low velocities implied by the narrow lines and the CSM-interaction are all consistent with SN 2009kn originating from a ECSN explosion of a super-AGB star with an initial mass close to the core-collapse limit ($\sim$8 $M_{\odot}$), that has lost a significant amount of mass shortly before the SN explosion. It seems that current stellar evolution models of some of the massive stars may require rework based on the studies of SN 2009kn-like events.

Early phase spectroscopic observations of SN 2009kn were carried out on my own initiative at the NOT, which demonstrated that this SN was a very rare and interesting event. Therefore, it became a high priority target for our wide European SN Collaboration. My contribution to the paper was data collection, reduction and analysis. I had the main role in writing the article.

6.2 Papers II & III

During the years 2008−2010 a sample of eight nearby ($\lesssim$ 100 Mpc) LIRGs was observed frequently in K-band high-resolution imaging to search for highly extinguished CCSNe and to obtain deep high quality near-IR images of these galaxies for detailed studies of their super star cluster populations. The search was conducted with the Gemini-North Telescope using the Near-InfraRed Imager and spectrometer (NIRI) with the ALTtitude conjugate

Adaptive optics for the InfraRed (ALTAIR) AO system in the LGS mode. The discoveries and the follow-up observations of SNe 2004iq and 2008cs in IRAS 17138-1017, and SNe 2010cu and 2011hi in IC 883 were presented in papers II and III, respectively.

After detecting a new SN, multi-epoch follow-up imaging was conducted including observations in *JHK* using ALTAIR/NIRI. In the absence of spectroscopy, light curve and colour information is crucial to infer an estimate for the SN type and the host galaxy extinction in the SN line-of-sight. Based on the comparison of the observed *JHK* light curves with the template light curves of different CCSNe, likely types and host galaxy line-of-sight extinctions were derived for these SNe. In paper II the two near-IR light curve templates from Mattila & Meikle (2001) were used for comparison and in paper III the same templates were used in addition to the *JHK* light curves of SN 1999em from Krisciunas et al. (2009) to represent a canonical Type IIP SN.

The increased statistics provided by new SN discoveries in LIRGs are crucial for better estimates of line-of-sight extinctions, properties of the SN population and finally the CCSN rates in these galaxies. These are all important ingredients that can be used in studies such as the one presented in paper V, probing the cosmic CCSN rate, SFR and therefore also the galaxy evolution.

I was responsible for reducing and analysing all the near-IR data in (almost) real time including image subtraction to discover the SNe. I carried out the photometry and comparison of the light curve data to the template light curves and derived likely types and host galaxy extinctions for the SNe. I had the main role in writing the articles.

6.3 Paper IV

In paper IV the optical depth of spiral galaxies was studied statistically using a method presented originally by Bottinelli et al. (1995). Both diameter and magnitude limited subsamples of galaxies, as free from selection effects as possible, were derived using this method. Based on the inclination dependence of the galaxy disk diameter, a relatively low optical depth of $\tau_B \approx 0.1$ was derived for the spiral galaxy disks. However, any inclination effects of the diameter are dominated by the optical depth in the outer parts of the galaxy disk, and therefore this optical depth is also most

representative of the outer parts of the galaxy disk. A similar method was also used for the inclination dependence of the total magnitudes of the galaxy subsample, and a lower limit of $\tau_B > 1$ was derived, representing the optical depth over the whole galaxy disk. This method becomes fairly uncertain with high optical depths ($\tau_B \gtrsim 1$) and therefore only a lower limit was given. Our result is fairly consistent with that previously obtained by Bottinelli et al. (1995) and can be explained as a radially declining extinction in the spiral galaxy disks, with significant extinction in the centre of the galaxy, even at low inclination angles.

By statistically giving estimates of the spiral galaxy extinctions, the work in paper IV is complementary, for example, to SN host galaxy extinction studies, such as the one presented in paper V. The method used in paper IV can also be considered more reliable than some other statistical studies, as it emphasizes a sample selection as free from selection effects as possible.

My contribution to the publication was to programme the software to analyse the available statistical data. I had the main role in writing the article.

6.4 Paper V

In paper V a volume-limited sample of 13 nearby CCSNe was constructed, including events within 12 Mpc discovered between 2000−2011, and excluding SNe in inclined ($i > 60°$) host galaxies. Galaxies within this volume can be considered representative of normal spiral galaxies. For this sample of SNe the host galaxy extinctions were available in the literature or in the case of SN 2005at, derived by us from the available data. For SNe 2002hh and 2009hd, relatively high host galaxy extinctions of $A_V \approx 4$ mag have been reported in the literature, and these SNe would have probably been missed by optical SN searches at greater distances. In addition, such high host galaxy extinctions seem inconsistent with the underlying smooth distribution of extinction expected in the galaxy disk (e.g. see paper IV). We compared the observed extinction distribution of our CCSN sample (excluding the two above-mentionend outliers) with the SN host galaxy extinction model of Riello & Patat (2005). The Monte Carlo model parametrizes exponential distribution for both the CCSNe and the dust distribution. The model is scaled, based on the optical depth of the spiral galaxy through the

core (i.e. at zero radius) when seen face-on, which Riello & Patat (2005) defined with a fixed value of 1.0. A scaling factor of $\tau_V(0) = 2.5$ was found to match our observed sample. This up-scaling of the model is consistent, for example, with the statistical study presented in paper IV. Considering the fraction of CCSNe with very high host galaxy extinctions, a missing fraction of 15^{+21}_{-10} % for normal spiral galaxies was derived.

As a second step, a nearby LIRG Arp 299 was used as a template to derive the missing fraction for LIRGs in general. Both IR data and radio observations were used to give a predicted range of 1.6−1.9 SNe yr^{-1} for the total CCSN rate in Arp 299. Such a nearby high SFR system has been the subject of continuous SN searches carried out by multiple groups at both optical and near-IR wavelengths. Based on the number of optically discovered SNe, a missing fraction of 83^{+9}_{-15} % was derived. Both CCSN rate and missing CCSN fractions were derived for the local Universe, and the local CCSN rate was found to be consistent with the expectations from the cosmic SFR. Next the missing fractions were extended as a function of redshift. The high-z CCSN rate studies of Melinder et al. (2012) and Dahlen et al. (2012) adopted the missing fractions presented in paper V, and their corrected SNRs were found to be consistent with the predicted SFR, also at high-z. Therefore, the effect of missing SNe due to high extinction, combined with a population of intrinsically faint SNe, was found to be capable of eliminating the 'supernova rate problem' identified by Horiuchi et al. (2011).

My contribution to the article was to develop the Monte Carlo code used to derive host galaxy extinction distributions for SNe in normal spiral galaxies. I also reduced and analysed the data of SN 2005at, and derived the host galaxy extinction of the SN to complete our sample of nearby CCSNe with extinction estimates. When the article was being prepared I actively took part in the discussions and made suggestions regarding the analysis.

Chapter 7

Future work

The research projects that I have been working on and that are presented in this thesis will continue in the future. Detailed follow-up studies of various kinds of Type IIn SNe will increase the knowledge of these peculiar events, helping to better understand their origin and progenitors. The follow-up work combined with various statistical studies, and future work on Type IIn progenitors that will be discovered with deep high-resolution pre-explosion images, will increase our knowledge of stellar evolution, and could led to the need for a review of the current models concerning the final stages of some of the most massive stars. Therefore, I plan to continue with the follow-up studies of CSM interacting CCSNe with special interest on rare and peculiar transients such as SN 2009kn-like events, which are not yet that well understood and covered in the literature.

Increased statistics of CCSNe discovered in LIRGs are required for numerous reasons. A detailed near-IR search for SNe with short enough cadence using adaptive optics is bound to significantly increase the number of CCSNe discovered in LIRGs. In particular, the next generation multi-conjugate AO systems, such as Gemini Multi-conjugate adaptive optics Systems (GeMS) at Gemini-South Telescope, or the planned MICADO/MAORY for the E-ELT with a number of laser and NGSs utilized simultaneously, will ensure a larger field-of-view (FOV) and a PSF spatially stable over the full FOV, over multiple exposures and multiple epochs, hence improving the quality of image subtraction and photometry.

Increased statistics can also be used to more accurately constrain the SNR in LIRGs. A detailed follow-up, using well sampled light curves and radio observations, can allow us to more confidentally classify these SNe. The questions concerning CCSN populations in LIRGs can also be better addressed with the help of improved statistics. In addition, the line-of-

sight extinctions derived for the SNe can be used to study the extinction distributions in LIRGs. This is extremely useful for studies of LIRGs and for deriving extinction corrections for SNe in LIRGs, which is crucial in high-z SNR work, itself being a key element in galaxy evolution. Therefore, I am very interested in continuing to research the CCSN populations of LIRGs using the most advanced observational methods and instruments available.

Finally, there is a lack of realistic models for extinction correction for CCSN rates in normal spiral galaxies. The new systematic SN surveys with increased statistics can be used to more accurately define and calibrate the parameters for Monte Carlo simulations, and to derive extinction corrections for use in SNR studies. My objective is to continue the work started in paper V by developing a new model for SN and dust distributions in normal spiral galaxies, using the most recent SN statistics provided, for example, by the LOSS, in order to derive an extinction correction model for SNe. There will soon be an obvious need for such a tool to derive accurate extinction corrections for SN searches, as new SNR studies from large scale high-z sky surveys, carried out, for example, with *JWST*, LSST and E-ELT are due to start in the near future.

Bibliography

Agnoletto, I., et al. 2009, ApJ, 691, 1348

Alard, C., & Lupton, R. H. 1998, ApJ, 503, 325

Alard, C. 2000, A&AS, 144, 363

Aldering, G., Antilogus, P., Bailey, S., et al. 2006, ApJ, 650, 510

Alonso-Herrero, A., Pereira-Santaella, M., Rieke, G. H., & Rigopoulou, D. 2012, ApJ, 744, 2

Anderson, J. P., & James, P. A. 2008, MNRAS, 390, 1527

Anderson, J. P., & James, P. A. 2009, MNRAS, 399, 559

Anderson, J. P., Habergham, S. M., & James, P. A. 2011, MNRAS, 416, 567

Anderson, J. P., Habergham, S. M., James, P. A., & Hamuy, M. 2012, MNRAS, 424, 1372

Arcavi, I., Gal-Yam, A., Kasliwal, M. M., et al. 2010, ApJ, 721, 777

Arcavi, I., Gal-Yam, A., Cenko, S. B., et al. 2012, ApJ, 756, L30

Arnett, W. D. 1979, ApJ, 230, L37

Arnett, W. D. 1982, ApJ, 253, 785

Barbon, R., Ciatti, F., & Rosino, L. 1979, A&A, 72, 287

Barbon, R., Cappellaro, E., & Turatto, M. 1984, A&A, 135, 27

Batejat, F., Conway, J. E., Hurley, R., et al. 2011, ApJ, 740, 95

Bazin, G., Palanque-Delabrouille, N., Rich, J., et al. 2009, A&A, 499, 653

Benetti, S., Cappellaro, E., Danziger, I. J., et al. 1998, MNRAS, 294, 448

Benetti, S., Turatto, M., Cappellaro, E., Danziger, I. J., & Mazzali, P. A. 1999, MNRAS, 305, 811

Benetti, S., Cappellaro, E., Turatto, M., et al. 2006, ApJ, 653, L129

Berger, E., Soderberg, A. M., Chevalier, R. A., et al. 2009, ApJ, 699, 1850

Bessell, M. S. 1990, PASP, 102, 1181

Bohlin, R. C., Savage, B. D., & Drake, J. F. 1978, ApJ, 224, 132

Bond, H. E., Bedin, L. R., Bonanos, A. Z., et al. 2009, ApJ, 695, L154

Bondi, M., Pérez-Torres, M. A., Herrero-Illana, R., & Alberdi, A. 2012, A&A, 539, A134

Botticella, M. T., Riello, M., Cappellaro, E., et al. 2008, A&A, 479, 49

Botticella, M. T., Pastorello, A., Smartt, S. J., et al. 2009, MNRAS, 398, 1041

Botticella, M. T., Smartt, S. J., Kennicutt, R. C., et al. 2012, A&A, 537, A132

Bottinelli, L., Gouguenheim, L., Paturel, G., & Teerikorpi, P. 1995, A&A, 296, 64

Bouchet, P., Phillips, M. M., Suntzeff, N. B., et al. 1991, A&A, 245, 490

Bowen, D. V., Roth, K. C., Meyer, D. M., & Blades, J. C. 2000, ApJ, 536, 225

Bramich, D. M. 2008, MNRAS, 386, L77

Calzetti, D., Armus, L., Bohlin, R. C., et al. 2000, ApJ, 533, 682

Cappellaro, E., Evans, R., & Turatto, M. 1999, A&A, 351, 459

Cappellaro, E., Patat, F., Mazzali, P. A., et al. 2001, ApJ, 549, L215

Cardelli, J. A., Clayton, G. C., & Mathis, J. S. 1989, ApJ, 345, 245

Chevalier, R. A., & Fransson, C. 1994, ApJ, 420, 268

Chevalier, R. A., & Soderberg, A. M. 2010, ApJ, 711, L40

Chugai, N. N., & Danziger, I. J. 1994, MNRAS, 268, 173

Chugai, N. N., et al. 2004, MNRAS, 352, 1213

Cohen, M., Wheaton, W. A., & Megeath, S. T. 2003, AJ, 126, 1090

Colgate, S. A., Petschek, A. G., & Kriese, J. T. 1980, ApJ, 237, L81

Crowther, P. A. 2007, ARA&A, 45, 177

Crowther, P. A. 2013, MNRAS, 428, 1927

Dahlén, T., & Fransson, C. 1999, A&A, 350, 349

Dahlen, T., Strolger, L.-G., Riess, A. G., et al. 2004, ApJ, 613, 189

Dahlen, T., Strolger, L.-G., & Riess, A. G. 2008, ApJ, 681, 462

Dahlen, T., Strolger, L.-G., Riess, A. G., et al. 2012, ApJ, 757, 70

Danchi, W. C., Bester, M., Degiacomi, C. G., Greenhill, L. J., & Townes, C. H. 1994, AJ, 107, 1469

Davies, R., & Kasper, M. 2012, ARA&A, 50, 305

Dessart, L., Hillier, D. J., Gezari, S., Basa, S., & Matheson, T. 2009, MNRAS, 394, 21

Dessart, L., Livne, E., & Waldman, R. 2010, MNRAS, 405, 2113

Diehl, R., & Timmes, F. X. 1998, PASP, 110, 637

Dilday, B., Smith, M., Bassett, B., et al. 2010, ApJ, 713, 1026

Dilday, B., Howell, D. A., Cenko, S. B., et al. 2012, Science, 337, 942

Doggett, J. B., & Branch, D. 1985, AJ, 90, 2303

Draine, B. T. 2003, ARA&A, 41, 241

Drout, M. R., Soderberg, A. M., Gal-Yam, A., et al. 2011, ApJ, 741, 97

Dwarkadas, V. V. 2005, ApJ, 630, 892

Dwarkadas, V. V. 2011, MNRAS, 412, 1639

Dwek, E. 1983, ApJ, 274, 175

Eldridge, J. J., & Tout, C. A. 2004, MNRAS, 353, 87

Elmhamdi, A., Danziger, I. J., Cappellaro, E., et al. 2004, A&A, 426, 963

Elvis, M., Marengo, M., & Karovska, M. 2002, ApJ, 567, L107

Evans, R. 1997, PASA, 14, 204

Fassia, A., Meikle, W. P. S., Vacca, W. D., et al. 2000, MNRAS, 318, 1093

Fassia, A., Meikle, W. P. S., Chugai, N., et al. 2001, MNRAS, 325, 907

Filippenko, A. V. 1988, AJ, 96, 1941

Filippenko, A. V. 1997, ARA&A, 35, 309

Filippenko, A. V., Li, W. D., Treffers, R. R., & Modjaz, M. 2001, IAU Colloq. 183: Small Telescope Astronomy on Global Scales, 246, 121

Flower, P. J. 1996, ApJ, 469, 355

Foley, R. J., Smith, N., Ganeshalingam, M., et al. 2007, ApJ, 657, L105

Foley, R. J., Berger, E., Fox, O., et al. 2011, ApJ, 732, 32

Fox, O. D., Chevalier, R. A., Skrutskie, M. F., et al. 2011, ApJ, 741, 7

Fransson, C., & Kozma, C. 2002, New Astronomy Reviews, 46, 487

Fransson, C., Chevalier, R. A., Filippenko, A. V., et al. 2002, ApJ, 572, 350

Fransson, C., Challis, P. M., Chevalier, R. A., et al. 2005, ApJ, 622, 991

Fruchter, A. S., Levan, A. J., Strolger, L., et al. 2006, Nature, 441, 463

Gal-Yam, A., Leonard, D. C., Fox, D. B., et al. 2007, ApJ, 656, 372

Gal-Yam, A., & Leonard, D. C. 2009, Nature, 458, 865

Gal-Yam, A., Mazzali, P., Ofek, E. O., et al. 2009, Nature, 462, 624

Gal-Yam, A. 2012, Science, 337, 927

Galama, T. J., Vreeswijk, P. M., van Paradijs, J., et al. 1998, Nature, 395, 670

Gehrels, N., Ramirez-Ruiz, E., & Fox, D. B. 2009, ARA&A, 47, 567

Gehrz, R. 1989, Interstellar Dust, 135, 445

Gerardy, C. L., Fesen, R. A., Nomoto, K., et al. 2002, ApJ, 575, 1007

Gliese, W., & Jahreiß, H. 1991, On: The Astronomical Data Center CD-ROM: Selected Astronomical Catalogs, Vol. I; L.E. Brotzmann, S.E. Gesser (eds.), NASA/Astronomical Data Center, Goddard Space Flight Center, Greenbelt, MD,

Goobar, A., & Leibundgut, B. 2011, Annual Review of Nuclear and Particle Science, 61, 251

Graham, J. R., Meikle, W. P. S., Selby, M. J., et al. 1983, Nature, 304, 709

Graham, J. R., & Meikle, W. P. S. 1986, MNRAS, 221, 789

Graur, O., Poznanski, D., Maoz, D., et al. 2011, MNRAS, 417, 916

Grebenev, S. A., Lutovinov, A. A., Tsygankov, S. S., & Winkler, C. 2012, Nature, 490, 373

Grossan, B., Spillar, E., Tripp, R., et al. 1999, AJ, 118, 705

Gutiérrez, J., Canal, R., & García-Berro, E. 2005, A&A, 435, 231

Habergham, S. M., Anderson, J. P., & James, P. A. 2010, ApJ, 717, 342

Habergham, S. M., James, P. A., & Anderson, J. P. 2012, MNRAS, 424, 2841

Habing, H. J. 1996, A&AR, 7, 97

Hakobyan, A. A., Mamon, G. A., Petrosian, A. R., Kunth, D., & Turatto, M. 2009, A&A, 508, 1259

Hamuy, M., Phillips, M. M., Suntzeff, N. B., et al. 2003, Nature, 424, 651

Hashimoto, M., Iwamoto, K., & Nomoto, K. 1993, ApJ, 414, L105

Hatano, K., Branch, D., & Deaton, J. 1998, ApJ, 502, 177

Heger, A., & Woosley, S. E. 2002, ApJ, 567, 532

Heger, A., Fryer, C. L., Woosley, S. E., Langer, N., & Hartmann, D. H. 2003, ApJ, 591, 288

Hendry, M. A., Smartt, S. J., Maund, J. R., et al. 2005, MNRAS, 359, 906

Herrero-Illana, R., Pérez-Torres, M. Á., & Alberdi, A. 2012, A&A, 540, L5

Hillebrandt, W., & Niemeyer, J. C. 2000, ARA&A, 38, 191

Hjorth, J., Sollerman, J., Møller, P., et al. 2003, Nature, 423, 847

Horiuchi, S., Beacom, J. F., Kochanek, C. S., et al. 2011, ApJ, 738, 154

Howell, D. A., Sullivan, M., Nugent, P. E., et al. 2006, Nature, 443, 308

Humphreys, R. M., & Davidson, K. 1994, PASP, 106, 1025

Humphreys, R. M., Bond, H. E., Bedin, L. R., et al. 2011, ApJ, 743, 118

Humphreys, R. M., Davidson, K., Jones, T. J., et al. 2012, ApJ, 760, 93

Höfner, S., & Dorfi, E. A. 1997, A&A, 319, 648

Iben, I., Jr., & Tutukov, A. V. 1984, ApJS, 54, 335

Inserra, C., Turatto, M., Pastorello, A., et al. 2011, MNRAS, 417, 261

Israel, H., Hessman, F. V., & Schuh, S. 2007, Astronomische Nachrichten, 328, 16

James, P. A., & Anderson, J. P. 2006, A&A, 453, 57

Janka, H.-T., Langanke, K., Marek, A., Martínez-Pinedo, G., Müller, B. 2007, PhR, 442, 38

Kankare, E., Mattila, S., Hentunen, V.-P., & Pastorello, A. 2009, CBET, 1692, 1

Kankare, E., Mattila, S., Wright, D., et al. 2011, CBET, 2952, 2

Kelly, P. L., Kirshner, R. P., & Pahre, M. 2008, ApJ, 687, 1201

Kelly, P. L., & Kirshner, R. P. 2012, ApJ, 759, 107

Kitaura, F. S., Janka, H.-T., & Hillebrandt, W. 2006, A&A, 450, 345

Kochanek, C. S., Szczygieł, D. M., & Stanek, K. Z. 2012, ApJ, 758, 142

Kotak, R., Meikle, W. P. S., Adamson, A., & Leggett, S. K. 2004, MNRAS, 354, L13

Kotak, R., & Vink, J. S. 2006, A&A, 460, L5

Krisciunas, K., Hamuy, M., Suntzeff, N. B., et al. 2009, AJ, 137, 34

Kuznetsova, N. V., & Connolly, B. M. 2007, ApJ, 659, 530

Langer, N., Hamann, W.-R., Lennon, M., et al. 1994, A&A, 290, 819

Leaman, J., Li, W., Chornock, R., & Filippenko, A. V. 2011, MNRAS, 412, 1419

Le Floc'h, E., Papovich, C., Dole, H., et al. 2005, ApJ, 632, 169

Leitherer, C. 1997, Luminous Blue Variables: Massive Stars in Transition, 120, 58

Leloudas, G., Sollerman, J., Levan, A. J., et al. 2010, A&A, 518, A29

Lenzen, R., Hartung, M., Brandner, W., et al. 2003, Proc. SPIE, 4841, 944

Leonard, D. C., Filippenko, A. V., Barth, A. J., & Matheson, T. 2000, ApJ, 536, 239

Li, W., Leaman, J., Chornock, R., et al. 2011a, MNRAS, 412, 1441

Li, W., Chornock, R., Leaman, J., et al. 2011b, MNRAS, 412, 1473

Li, W., Bloom, J. S., Podsiadlowski, P., et al. 2011c, Nature, 480, 348

Liu, Q.-Z., Hu, J.-Y., Hang, H.-R., et al. 2000, A&AS, 144, 219

Lonsdale, C. J., Diamond, P. J., Thrall, H., Smith, H. E., & Lonsdale, C. J. 2006, ApJ, 647, 185

Lucy, L. B., Danziger, I. J., Gouiffes, C., & Bouchet, P. 1989, IAU Colloq. 120: Structure and Dynamics of the Interstellar Medium, 350, 164

MacFadyen, A. I., & Woosley, S. E. 1999, ApJ, 524, 262

Maeder, A., & Conti, P. S. 1994, ARA&A, 32, 227

Magnelli, B., Elbaz, D., Chary, R. R., et al. 2009, A&A, 496, 57

Magnelli, B., Elbaz, D., Chary, R. R., et al. 2011, A&A, 528, A35

Maiolino, R., Vanzi, L., Mannucci, F., et al. 2002, A&A, 389, 84

Mannucci, F., Maiolino, R., Cresci, G., et al. 2003, A&A, 401, 519

Mannucci, F., Della Valle, M., & Panagia, N. 2007, MNRAS, 377, 1229

Mattila, S., & Meikle, W. P. S. 2001, MNRAS, 324, 325

Mattila, S., Meikle, W. P. S., & Greimel, R. 2004, New Astronomy Reviews, 48, 595

Mattila, S., Väisänen, P., Farrah, D., et al. 2007, ApJ, 659, L9

Mattila, S., Meikle, W. P. S., Lundqvist, P., et al. 2008, MNRAS, 389, 141

Mauerhan, J. C., Smith, N., Silverman, J. M., et al. 2012, arXiv:1209.0821

Maund, J. R., Smartt, S. J., Kudritzki, R. P., Podsiadlowski, P., & Gilmore, G. F. 2004, Nature, 427, 129

Maund, J. R., Smartt, S. J., Kudritzki, R.-P., et al. 2006, MNRAS, 369, 390

Maund, J. R., & Smartt, S. J. 2009, Science, 324, 486

Maund, J. R., Fraser, M., Ergon, M., et al. 2011, ApJ, 739, L37

Mayle, R., & Wilson, J. R. 1988, ApJ, 334, 909

Meikle, W. P. S., Mattila, S., Pastorello, A., et al. 2007, ApJ, 665, 608

Melinder, J., Mattila, S., Östlin, G., Mencía Trinchant, L., & Fransson, C. 2008, A&A, 490, 419

Melinder, J., Dahlen, T., Mencía-Trinchant, L., et al. 2011, A&A, 532, A29

Melinder, J., Dahlen, T., Mencía Trinchant, L., et al. 2012, A&A, 545, A96

Miyaji, S., Nomoto, K., Yokoi, K., & Sugimoto, D. 1980, PASJ, 32, 303

Miyaji, S., & Nomoto, K. 1987, ApJ, 318, 307

Nomoto, K. 1982, ApJ, 253, 798

Nomoto, K. 1984, ApJ, 277, 791

Nomoto, K. 1987, ApJ, 322, 206

Ochsenbein, F., Bauer, P., & Marcout, J. 2000, A&AS, 143, 23

Osterbrock, D. E., & Ferland, G. J. 2006, Astrophysics of gaseous nebulae and active galactic nuclei, 2nd. ed. by D.E. Osterbrock and G.J. Ferland. Sausalito, CA: University Science Books, 2006,

Parra, R., Conway, J. E., Diamond, P. J., et al. 2007, ApJ, 659, 314

Pastorello, A., Sauer, D., Taubenberger, S., et al. 2006, MNRAS, 370, 1752

Pastorello, A., Smartt, S. J., Mattila, S., et al. 2007, Nature, 447, 829

Pastorello, A., Mattila, S., Zampieri, L., et al. 2008, MNRAS, 389, 113

Pastorello, A., Valenti, S., Zampieri, L., et al. 2009, MNRAS, 394, 2266

Pastorello, A., Botticella, M. T., Trundle, C., et al. 2010, MNRAS, 408, 181

Pastorello, A., Benetti, S., Bufano, F., et al. 2011, Astronomische Nachrichten, 332, 266

Pastorello, A., Cappellaro, E., Inserra, C., et al. 2012, arXiv:1210.3568

Pérez-Torres, M. A., Romero-Cañizales, C., Alberdi, A., & Polatidis, A. 2009, A&A, 507, L17

Perlmutter, S., Aldering, G., Goldhaber, G., et al. 1999, ApJ, 517, 565

Perryman, M. A. C., Lindegren, L., Kovalevsky, J., et al. 1997, A&A, 323, L49

Petrosian, A., Navasardyan, H., Cappellaro, E., et al. 2005, AJ, 129, 1369

Phillips, M. M. 1993, ApJ, 413, L105

Podsiadlowski, P., Joss, P. C., & Hsu, J. J. L. 1992, ApJ, 391, 246

Poelarends, A. J. T., Herwig, F., Langer, N., & Heger, A. 2008, ApJ, 675, 614

Pooley, D., Lewin, W. H. G., Fox, D. W., et al. 2002, ApJ, 572, 932

Poznanski, D., Gal-Yam, A., Maoz, D., et al. 2002, PASP, 114, 833

Poznanski, D., Maoz, D., & Gal-Yam, A. 2007, AJ, 134, 1285

Poznanski, D., Ganeshalingam, M., Silverman, J. M., & Filippenko, A. V. 2011, MNRAS, 415, L81

Poznanski, D., Prochaska, J. X., & Bloom, J. S. 2012, MNRAS, 426, 1465

Pozzo, M., Meikle, W. P. S., Fassia, A., et al. 2004, MNRAS, 352, 457

Prantzos, N., & Boissier, S. 2003, A&A, 406, 259

Prieto, J. L., Garnavich, P. M., Phillips, M. M., et al. 2007, arXiv:0706.4088

Prieto, J. L., Kistler, M. D., Thompson, T. A., et al. 2008, ApJ, 681, L9

Richardson, D., Branch, D., Casebeer, D., et al. 2002, AJ, 123, 745

Rieke, G. H., & Lebofsky, M. J. 1985, ApJ, 288, 618

Riello, M., & Patat, F. 2005, MNRAS, 362, 671

Riess, A. G., Press, W. H., & Kirshner, R. P. 1996, ApJ, 473, 88

Riess, A. G., Filippenko, A. V., Challis, P., et al. 1998, AJ, 116, 1009

Rodney, S. A., & Tonry, J. L. 2010, ApJ, 723, 47

Roming, P. W. A., Pritchard, T. A., Prieto, J. L., et al. 2012, ApJ, 751, 92

Rousset, G., Lacombe, F., Puget, P., et al. 2003, Proc. SPIE, 4839, 140

Salpeter, E. E. 1955, ApJ, 121, 161

Sanders, D. B., & Mirabel, I. F. 1996, ARA&A, 34, 749

Scannapieco, E., Madau, P., Woosley, S., Heger, A., & Ferrara, A. 2005, ApJ, 633, 1031

Schlafly, E. F., & Finkbeiner, D. P. 2011, ApJ, 737, 103

Schlegel, E. M. 1990, MNRAS, 244, 269

Schlegel, D. J., Finkbeiner, D. P., & Davis, M. 1998, ApJ, 500, 525

Scoville, N. Z., Evans, A. S., Thompson, R., et al. 2000, AJ, 119, 991

Smartt, S. J. 2009, ARA&A, 47, 63

Smartt, S. J., Eldridge, J. J., Crockett, R. M., & Maund, J. R. 2009, MNRAS, 395, 1409

Smith, N., & McCray, R. 2007, ApJ, 671, L17

Smith, N., et al. 2007, ApJ, 666, 1116

Smith, N., Foley, R. J., Bloom, J. S., et al. 2008a, ApJ, 686, 485

Smith, N., Foley, R. J., & Filippenko, A. V. 2008b, ApJ, 680, 568

Smith, N., Ganeshalingam, M., Chornock, R., et al. 2009a, ApJ, 697, L49

Smith, N., Hinkle, K. H., & Ryde, N. 2009b, AJ, 137, 3558

Smith, N., Silverman, J. M., Chornock, R., et al. 2009c, ApJ, 695, 1334

Smith, N., Chornock, R., Silverman, J. M., Filippenko, A. V., & Foley, R. J. 2010a, ApJ, 709, 856

Smith, N., Miller, A., Li, W., et al. 2010b, AJ, 139, 1451

Smith, N., Li, W., Filippenko, A. V., & Chornock, R. 2011a, MNRAS, 412, 1522

Smith, N., Li, W., Miller, A. A., et al. 2011b, ApJ, 732, 63

Smith, N., Li, W., Silverman, J. M., Ganeshalingam, M., & Filippenko, A. V. 2011c, MNRAS, 415, 773

Soifer, B. T., Neugebauer, G., Matthews, K., et al. 2001, AJ, 122, 1213

Stathakis, R. A., & Sadler, E. M. 1991, MNRAS, 250, 786

Sugerman, B. E. K., Andrews, J. E., Barlow, M. J., et al. 2012, ApJ, 749, 170

Szalai, T., Vinkó, J., Balog, Z., et al. 2011, A&A, 527, A61

Taddia, F., Stritzinger, M. D., Phillips, M. M., et al. 2012, A&A, 545, L7

Taubenberger, S., Valenti, S., Benetti, S., et al. 2009, MNRAS, 397, 677

Thompson, T. A., Prieto, J. L., Stanek, K. Z., et al. 2009, ApJ, 705, 1364

Trundle, C., Kotak, R., Vink, J. S., & Meikle, W. P. S. 2008, A&A, 483, L47

Turatto, M., Cappellaro, E., Danziger, I. J., et al. 1993, MNRAS, 262, 128

Turatto, M., Suzuki, T., Mazzali, P. A., et al. 2000, ApJ, 534, L57

Turatto, M., Benetti, S., & Cappellaro, E. 2003, From Twilight to Highlight: The Physics of Supernovae, 200

Ulvestad, J. S. 2009, AJ, 138, 1529

Van Dyk, S. D., Li, W., Cenko, S. B., et al. 2011, ApJ, 741, L28

Wagner, R. M., Vrba, F. J., Henden, A. A., et al. 2004, PASP, 116, 326

Waldman, R. 2008, ApJ, 685, 1103

Walmswell, J. J., & Eldridge, J. J. 2012, MNRAS, 419, 2054

Wanajo, S., Nomoto, K., Janka, H.-T., Kitaura, F. S., Müller, B. 2009, ApJ, 695, 208

Weaver, T. A., & Woosley, S. E. 1979, BAAS, 11, 724

Webbink, R. F. 1984, ApJ, 277, 355

Weis, K., & Bomans, D. J. 2005, A&A, 429, L13

Whelan, J., & Iben, I., Jr. 1973, ApJ, 186, 1007

Woosley, S. E., & Weaver, T. A. 1986, ARA&A, 24, 205

Woosley, S. E., Pinto, P. A., Martin, P. G., & Weaver, T. A. 1987, ApJ, 318, 664

Woosley, S. E., Pinto, P. A. & Hartmann, D. 1989, ApJ, 346, 395

Woosley, S. E., Heger, A., & Weaver, T. A. 2002, Reviews of Modern Physics, 74, 1015

Woosley, S. E., & Bloom, J. S. 2006, ARA&A, 44, 507

Woosley, S. E., Blinnikov, S., & Heger, A. 2007, Nature, 450, 390

Yoon, S.-C., & Cantiello, M. 2010, ApJ, 717, L62

Yuan, F., & Akerlof, C. W. 2008, ApJ, 677, 808